Gohl, K., Wellner, J.S., Klaus, A., and the Expedition 379 Scientists
Proceedings of the International Ocean Discovery Program Volume 379
publications.iodp.org

https://doi.org/10.14379/iodp.proc.379.101.2021

Check for updates

Expedition 379 summary[1]

K. Gohl, J.S. Wellner, A. Klaus, T. Bauersachs, S.M. Bohaty, M. Courtillat, E.A. Cowan, M.A. De Lira Mota, M.S.R. Esteves, J.M. Fegyveresi, T. Frederichs, L. Gao, A.R. Halberstadt, C.-D. Hillenbrand, K. Horikawa, M. Iwai, J.-H. Kim, T.M. King, J.P. Klages, S. Passchier, M.L. Penkrot, J.G. Prebble, W. Rahaman, B.T.I. Reinardy, J. Renaudie, D.E. Robinson, R.P. Scherer, C.S. Siddoway, L. Wu, and M. Yamane[2]

Keywords: Keywords: International Ocean Discovery Program, IODP, *JOIDES Resolution*, Expedition 379, Amundsen Sea West Antarctic Ice Sheet History, Site U1532, Site U1533, Amundsen Sea Embayment, Pine Island Glacier, Thwaites Glacier, Marie Byrd Land, paleoclimate, paleo–ice sheet, marine ice sheet, continental rise, deep-sea sediments, sediment drift, contourite, ocean-bottom current, seismic stratigraphy, ice-rafted debris, glacial–interglacial cyclicity, core X-ray, headspace gas, contamination tracer

Contents

Abstract

The Amundsen Sea sector of Antarctica has long been considered the most vulnerable part of the West Antarctic Ice Sheet (WAIS) because of the great water depth at the grounding line, a subglacial bed seafloor deepening toward the interior of the continent, and the absence of substantial ice shelves. Glaciers in this configuration are thought to be susceptible to rapid or runaway retreat. Ice flowing into the Amundsen Sea Embayment is undergoing the most rapid changes of any sector of the Antarctic ice sheets outside the Antarctic Peninsula, including substantial grounding-line retreat over recent decades, as observed from satellite data. Recent models suggest that a threshold leading to the collapse of WAIS in this sector may have been already crossed and that much of the ice sheet could be lost even under relatively moderate greenhouse gas emission scenarios.

Drill cores from the Amundsen Sea provide tests of several key questions about controls on ice sheet stability. The cores offer a direct offshore record of glacial history in a sector that is exclusively influenced by ice draining the WAIS, which allows clear comparisons between the WAIS history and low-latitude climate records. Today, relatively warm (modified) Circumpolar Deep Water (CDW) is impinging onto the Amundsen Sea shelf and causing melting under ice shelves and at the grounding line of the WAIS in most places. Reconstructions of past CDW intrusions can assess the ties between warm water upwelling and large-scale changes in past grounding-line positions. Carrying out these reconstructions offshore from the drainage basin that currently has the most substantial negative mass balance of ice anywhere in Antarctica is thus of prime interest to future predictions.

The scientific objectives for this expedition are built on hypotheses about WAIS dynamics and related paleoenvironmental and paleoclimatic conditions. The main objectives are

1. To test the hypothesis that WAIS collapses occurred during the Neogene and Quaternary and, if so, when and under which environmental conditions;
2. To obtain ice-proximal records of ice sheet dynamics in the Amundsen Sea that correlate with global records of ice-volume changes and proxy records for atmospheric and ocean temperatures;
3. To study the stability of a marine-based WAIS margin and how warm deepwater incursions control its position on the shelf;
4. To find evidence for the earliest major grounded WAIS advances onto the middle and outer shelf;
5. To test the hypothesis that the first major WAIS growth was related to the uplift of the Marie Byrd Land dome.

International Ocean Discovery Program (IODP) Expedition 379 completed two very successful drill sites on the continental rise of the Amundsen Sea. Site U1532 is located on a large sediment drift, now called the Resolution Drift, and it penetrated to 794 m with 90% recovery. We collected almost-continuous cores from recent age through the Pleistocene and Pliocene and into the upper Mio-

[1] Gohl, K., Wellner, J.S., Klaus, A., Bauersachs, T., Bohaty, S.M., Courtillat, M., Cowan, E.A., De Lira Mota, M.A., Esteves, M.S.R., Fegyveresi, J.M., Frederichs, T., Gao, L., Halberstadt, A.R., Hillenbrand, C.-D., Horikawa, K., Iwai, M., Kim, J.-H., King, T.M., Klages, J.P., Passchier, S., Penkrot, M.L., Prebble, J.G., Rahaman, W., Reinardy, B.T.I., Renaudie, J., Robinson, D.E., Scherer, R.P., Siddoway, C.S., Wu, L., and Yamane, M., 2021. Expedition 379 summary. *In* Gohl, K., Wellner, J.S., Klaus, A., and the Expedition 379 Scientists, *Amundsen Sea West Antarctic Ice Sheet History.* Proceedings of the International Ocean Discovery Program, 379: College Station, TX (International Ocean Discovery Program). https://doi.org/10.14379/iodp.proc.379.101.2021

[2] **Expedition 379 Scientists' affiliations.**

MS 379-101: Published 23 February 2021

cene. At Site U1533, we drilled 383 m (70% recovery) into the more condensed sequence at the lower flank of the same sediment drift. The cores of both sites contain unique records that will enable study of the cyclicity of ice sheet advance and retreat processes as well as ocean-bottom water circulation and water mass changes. In particular, Site U1532 revealed a sequence of Pliocene sediments with an excellent paleomagnetic record for high-resolution climate change studies of the previously sparsely sampled Pacific sector of the West Antarctic margin.

Despite the drilling success at these sites, the overall expedition experienced three unexpected difficulties that affected many of the scientific objectives:

1. The extensive sea ice on the continental shelf prevented us from drilling any of the proposed shelf sites.
2. The drill sites on the continental rise were in the path of numerous icebergs of various sizes that frequently forced us to pause drilling or leave the hole entirely as they approached the ship. The overall downtime caused by approaching icebergs was 50% of our time spent on site.
3. A medical evacuation cut the expedition short by 1 week.

Recovery of core on the continental rise at Sites U1532 and U1533 cannot be used to indicate the extent of grounded ice on the shelf or, thus, of its retreat directly. However, the sediments contained in these cores offer a range of clues about past WAIS extent and retreat. At Sites U1532 and U1533, coarse-grained sediments interpreted to be ice-rafted debris (IRD) were identified throughout all recovered time periods. A dominant feature of the cores is recorded by lithofacies cyclicity, which is interpreted to represent relatively warmer periods variably characterized by sediments with higher microfossil abundance, greater bioturbation, and higher IRD concentrations alternating with colder periods characterized by dominantly gray laminated terrigenous muds. Initial comparison of these cycles to published late Quaternary records from the region suggests that the units interpreted to be records of warmer time intervals in the core tie to global interglacial periods and the units interpreted to be deposits of colder periods tie to global glacial periods.

Cores from the two drill sites recovered sediments of dominantly terrigenous origin intercalated or mixed with pelagic or hemipelagic deposits. In particular, Site U1533, which is located near a deep-sea channel originating from the continental slope, contains graded silts, sands, and gravels transported downslope from the shelf to the rise. The channel is likely the pathway of these sediments transported by turbidity currents and other gravitational downslope processes. The association of lithologic facies at both sites predominantly reflects the interplay of downslope and contouritic sediment supply with occasional input of more pelagic sediment. Despite the lack of cores from the shelf, our records from the continental rise reveal the timing of glacial advances across the shelf and thus the existence of a continent-wide ice sheet in West Antarctica during longer time periods since at least the late Miocene.

Cores from both sites contain abundant coarse-grained sediments and clasts of plutonic origin transported either by downslope processes or by ice rafting. If detailed provenance studies confirm our preliminary assessment that the origin of these samples is from the plutonic bedrock of Marie Byrd Land, their thermochronological record will potentially reveal timing and rates of denudation and erosion linked to crustal uplift. The chronostratigraphy of both sites enables the generation of a seismic sequence stratigraphy for the entire Amundsen Sea continental rise, spanning the area offshore from the Amundsen Sea Embayment westward along the Marie Byrd Land margin to the easternmost Ross Sea through a connecting network of seismic lines.

Introduction

For decades, the drainage basins feeding ice into the Amundsen Sea have been considered the most vulnerable part of the mostly marine based West Antarctic Ice Sheet (WAIS) because of the great water depth at the grounding line, a subglacial bed deepening toward the interior of the continent, and the lack of substantial buttressing ice shelves (Hughes, 1981). Glaciers in this configuration are thought to be susceptible to rapid or runaway retreat (Schoof, 2007). Ice flowing into the Amundsen Sea Embayment is undergoing the most rapid changes of any sector of the Antarctic Ice Sheet, including substantial grounding line retreat over recent decades, as observed from satellite data (e.g., Milillo et al., 2019). Recent models suggest that a threshold leading to a (partial) collapse of the WAIS in this sector may have been passed already (Joughin et al., 2014) and that much of the ice sheet could be lost even under relatively moderate greenhouse gas emission scenarios (DeConto and Pollard, 2016). Model projections are limited by a lack of constraints in several areas, most notably in a lack of detailed reconstructions of glacial history, which is only constrained for the time since the Last Glacial Maximum (LGM; Larter et al., 2014; Smith et al., 2014).

Drill cores from the Amundsen Sea (Figure **F1**) provide tests of several key questions about controls on ice sheet stability. First, the cores offer a direct record of glacial history in a drainage basin that receives ice only from the WAIS and thus allow clear comparisons between the WAIS history and low-latitude climate records. Most ice draining into the Amundsen Sea is grounded below sea level; thus, a complete and well-dated sedimentary record offshore can

Figure F1. Eastern Amundsen Sea continental shelf and rise bathymetry. Red stars mark Expedition 379 sites on the Resolution Drift (RD), which is one of five large north–northeast-striking sediment drift bodies on the rise. Green circles show the location of Proposal 839 primary and alternate drill sites. Gray lines show the location of existing seismic lines. Annotated glacial troughs on the shelf are Dotson-Getz Trough (DGT), Pine Island Trough West (PITW), Pine Island Trough East (PITE), Pine Island Trough Central (PITC), and Abbot Trough (AT).

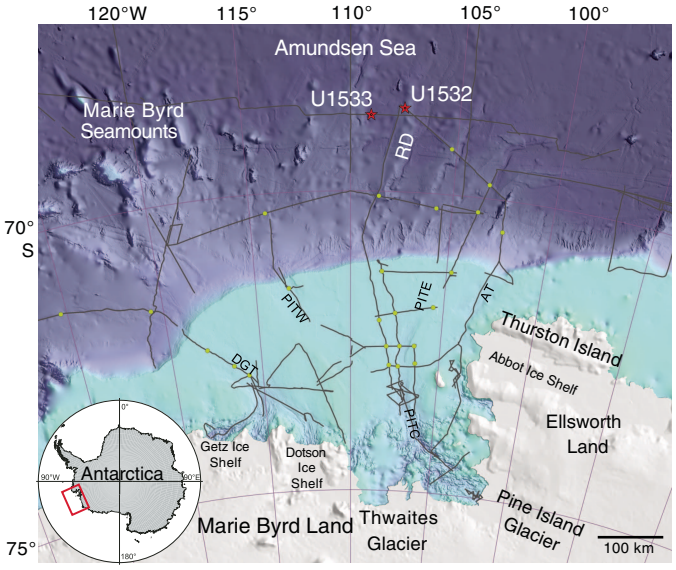

provide a direct link between WAIS growth and decay and global climate and sea-level records, offering a test of the marine ice sheet instability. Today, warm (modified) Circumpolar Deep Water (CDW) impinges onto the Amundsen Sea shelf, which causes melting under ice shelves and at the grounding line in some places (Millillo et al., 2019). Reconstructions of past CDW intrusions (Hillenbrand et al., 2017; Minzoni et al., 2017) can assess the ties between warm water and large-scale changes in past grounding-line positions. Carrying out these reconstructions offshore from the drainage basin that currently has the largest negative mass balance of ice of anywhere in Antarctica (Paolo et al., 2015) is thus of prime interest to future predictions. Finally, Expedition 379 is part of a suite of International Ocean Discovery Program (IODP) expeditions in the Antarctic that allow large-scale reconstructions and comparisons between different drainage basins.

Background

The fourth assessment report of the Intergovernmental Panel on Climate Change (IPCC) (2007) already highlighted the fact that the response of continental ice sheets to climatic changes and their contribution to global sea level change is the largest unknown variable in predicting future sea level change. The fifth assessment report of the IPCC (2013) included more information about the likely contributions to sea level change from the Antarctic, but these contributions remain one of the primary unknowns in predictions of future change. Also, the 2013 IPCC assessment report emphasized that if there is a substantial increase in the rate of sea level rise in the next century, it is likely to come from marine-based ice like that in the Amundsen Sea Embayment. The recent Special Report on Global Warming of 1.5°C of the IPCC (2018) concluded that marine ice sheet instability in Antarctica and the irreversible loss of the Greenland Ice Sheet could be triggered by ~1.5° to 2°C of global warming and could result in multimeter sea level rise over hundreds to thousands of years.

The WAIS rests on a subglacial bed that typically deepens toward the interior of the Antarctic continent as a continuation of the fore-deepened continental shelf. Thus, the base of the ice is mostly positioned below sea level ("marine based"), and the WAIS is sensitive to global sea level rise and regional oceanographic and atmospheric changes, so its history has been highly dynamic (e.g., Joughin and Alley, 2011). A complete WAIS collapse would raise the global sea level by 3.3 to 4.3 m (Fretwell et al., 2013), whereas the collapse of its Amundsen Sea drainage sector would raise the sea level by ~1.5 m (Vaughan, 2008). Over the most recent decades, glaciers draining into the Amundsen Sea thinned at a rapid rate, their flow speed dramatically increased, and their grounding lines retreated significantly, thereby contributing to present sea level rise at a faster rate than from any other glacier on Earth (e.g., Joughin and Alley, 2011; Joughin et al., 2012; Paolo et al., 2015; Rignot et al., 2019).

The present ice loss in the Amundsen Sea region is mainly attributed to sub–ice shelf melting induced by relatively warm CDW upwelling onto the shelf and spreading through deep bathymetric troughs toward the grounding zones (e.g., Arneborg et al., 2012; Joughin et al., 2012). It is unclear, however, whether the current ice loss results from recent climatic/oceanographic warming or recent internal ice sheet dynamics (Joughin and Alley, 2011; Joughin et al., 2012). If the WAIS has undergone similar thinning and retreat in the past, the factors driving that retreat can be compared to modern conditions.

The reconstruction and quantification of WAIS collapse during the Neogene and Quaternary will provide constraints for ice sheet models (Figure **F2**) that predict future WAIS behavior and resulting sea level rise. Numerous modeling studies have tried to link the waxing and waning of the WAIS to various forcing mechanisms (e.g., Pollard and DeConto, 2009; Holden et al., 2010; DeConto and Pollard, 2016; Sutter et al., 2016). However, large uncertainties exist regarding the spatial and temporal variability of past ice sheet advance and retreat. These uncertainties are mainly caused by the lack of data from cores drilled proximal to the WAIS. The only existing drill cores along the Pacific Antarctic margin outside the Ross Sea are from Deep Sea Drilling Project (DSDP) Leg 35 in the Bellingshausen Sea (Hollister and Craddock, 1976) and Ocean Drilling Program (ODP) Leg 178 on the Antarctic Peninsula margin (Barker and Camerlenghi, 2002). Results from Leg 178 Site 1097, drilled on the

Figure F2. Antarctic ice sheet models for the Pliocene (modified from DeConto and Pollard, 2016) and the Last Interglacial (modified from Sutter et al., 2016) simulating the collapse of the WAIS in each of these two warm times. Major ice retreat in the Amundsen Sea Embayment (ASE) seems to be a precursor for partial or total WAIS collapse.

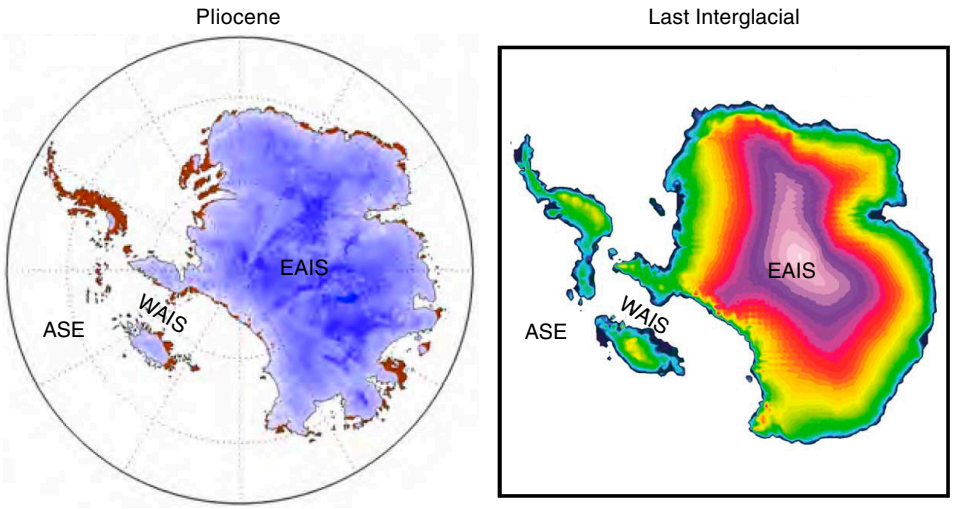

shelf, revealed a late Miocene age for the significant change in sequence geometry on the outer shelf that may indicate a change in the typical extent of glacial advances, the dynamic behavior of ice streams, or glacial sediment transport (Barker and Camerlenghi, 2002; Bart et al., 2005; Larter et al., 1997). Scheuer et al. (2006a, 2006b) were able to correlate seismic horizons on the western Antarctic Peninsula continental rise, which had been targeted by Leg 178 Sites 1095 and 1096 and were interpreted as transitions from preglacial to intermediate- and full-glacial conditions, from the eastern Bellingshausen Sea to the Amundsen Sea.

The most detailed results on Neogene WAIS history stem from the Antarctic Drilling Project (ANDRILL) in the western Ross Sea, which recovered early Miocene (~20 Ma) to Quaternary sequences in Cores AND-1B (Naish et al., 2009) and AND-2A (Passchier et al., 2011). Pliocene data from Core AND-1B indicate that orbitally induced oscillations of the WAIS resulted in transitions from grounded ice or ice shelves to open-water conditions (Naish et al., 2009; McKay et al., 2012). However, previous seismic stratigraphic work on the Ross Sea shelf beyond Site AND-1B revealed only seven shelf-wide grounding events (Alonso et al., 1992). Given the location of Site AND-1B, which is in a position to be overridden by both the East Antarctic Ice Sheet (EAIS) and the WAIS, the ANDRILL results are probably not representative of the WAIS outlets in the Amundsen, Bellingshausen, and Weddell Seas. Sedimentary records from the Ross and Weddell Seas provide only an integrated archive of WAIS and EAIS dynamics, whereas records from the Amundsen Sea will provide an unambiguous WAIS signal. We expect that results from recent IODP Expedition 374 to the Ross Sea shelf and slope will provide further insight into the WAIS dynamics for the Ross Sea sector (McKay et al., 2019). Although both the Ross Ice Shelf and the Filchner-Ronne Ice Shelf in the Weddell Sea extend far south, making positions proximal to the WAIS grounding-line difficult to access by drilling, only small and narrow ice shelves exist in the Amundsen Sea Embayment today.

Oceanographic setting

Persistent sea ice cover characterizes Pine Island Bay and the wider Amundsen Sea Embayment (e.g., Jacobs et al., 2012), and although sea ice cover has decreased significantly in recent decades (Parkinson and Cavalieri, 2012), 2018 and 2019 did not follow this trend; the sea ice cover of the Amundsen Sea was extensive throughout the entire austral summer and fall. Very little data on tidal ranges exist for the Amundsen Sea, but models suggest a 40 cm tidal height, making the area microtidal (Padman et al., 2002). Water mass temperatures within Pine Island Bay typically range between −1.5° and 0°C. The exception to this is warm CDW, which can reach temperatures of 1.5°C, that impinges onto the shelf through deep glacially carved troughs (Walker et al., 2007; Jacobs et al., 2011, 2013) and reaches the inner shelf in Pine Island Bay and offshore from the Dotson and westernmost Getz ice shelves (Jacobs et al., 2011, 2013) as well as, at times, smaller bays and fjords along the eastern coast of the Amundsen Sea Embayment (Minzoni et al., 2017). Productivity in polynyas in the Amundsen Sea is among the highest in the Southern Ocean and includes phytoplankton blooms (Arrigo et al., 2008, 2015; Minzoni et al., 2017). CDW-induced subice shelf melting is widely considered to be the primary external driver of contemporary glacier retreat in the Amundsen Sea, and recent work has shown that it can vary on seasonal (Kim et al., 2017) to decadal (Thoma et al., 2008; Dutrieux et al., 2014; Jenkins et al., 2016) timescales in response to wind stress at the continental shelf edge.

Geological setting

Together, ice sheet dynamics and tectonic and other geologic processes have shaped the Amundsen Sea continental shelf and rise. A 500–700 m deep shelf is incised by two major paleo–ice stream troughs, Pine Island Trough in the eastern Amundsen Sea Embayment and Dotson-Getz Trough in the western Amundsen Sea Embayment, whose tributaries originate from ice streams/glaciers on the innermost ultradeep (as deep as 1600 meters below sea level) shelf and converge at the transition from the inner to middle shelf (Lowe and Anderson, 2002; Larter et al., 2009; Graham et al., 2009, 2010). Both troughs extend toward the outer shelf, thereby becoming shallower and wider. The shelf geometry consists of a large pre- and synrift basin on the midshelf between the basement cropping out on the inner shelf and the buried basement highs on the outer shelf (Lowe and Anderson, 2002; Hochmuth and Gohl, 2013; Gohl et al., 2013b). A subordinate basin within the large midshelf basin may be associated with motion along an early West Antarctic Rift System branch. At least 4 km of preglacial strata were eroded by ice from the present inner shelf and coastal hinterland. At least five major erosional unconformities indicate phases of significant WAIS advances (Gohl et al., 2013b). Prograding sequences and subglacial bedforms on the outer shelf, subglacial tills recovered in cores, and radiocarbon dates on calcareous microfossils and organic matter in overlying sediments indicate that ground ice expanded to the outer shelf during the LGM and earlier glacial periods (Larter et al., 2014).

The continental rise is dominated by thick sedimentary deposition centers and by sediment drifts, both of which indicate strong bottom-current activity. Seismic data analyses from the Amundsen Sea rise suggest that sediment drift formation began in the Eocene/Oligocene (Uenzelmann-Neben and Gohl, 2012, 2014) (Figure **F3**). This implies bottom-current activity and hence a cold climate for the late Paleogene in the area that today probably lies under the influence of Antarctic Bottom Water originating in the Ross Sea. Seismic records from the continental rise along the entire Marie Byrd Land margin mark the base of the sediment drifts throughout the Amundsen Sea and into the Ross Sea (Lindeque et al., 2016a, 2016b). These records provide insight into sedimentation processes from preglacial to glacial times, variations in bottom-water circulation, early ice sheet growth, and glacial intensification toward the present icehouse regime (Uenzelmann-Neben and Gohl, 2012, 2014). However, stratigraphic age estimates are derived from long-distance seismic correlation with the western Antarctic Peninsula margin and the Ross Sea margin, and they hamper this insight.

Seismic records from the Amundsen Sea shelf show dipping strata on the midshelf that are possibly of Cretaceous to Miocene age and buried by aggradational, less consolidated strata of presumed Pliocene–Pleistocene age (Lowe and Anderson, 2002; Gohl et al., 2013b). Preliminary results from a seabed drilling expedition place constraints on the Cretaceous sequences that overlie outcropping bedrock on the middle and inner shelf in Pine Island Trough (Gohl et al., 2017). Since the mid-Miocene, the outer shelf and slope have undergone first progradational and then aggradational deposition (Nitsche et al., 1997; Hochmuth and Gohl, 2013; Gohl et al., 2013b). Several unconformities that possibly indicate phases of subglacial erosion and ice advance separate the dipping strata. Although most of the inner Amundsen Sea shelf is void of significant sedimentary cover (Lowe and Anderson, 2003; Graham et al., 2009; Gohl et al., 2013a, 2013b), a few small, shallow sediment basins lie along its eastern border (Uenzelmann-Neben et al., 2007) and in front of Pine Island Glacier (Nitsche et al., 2013; Muto et al., 2016).

Figure F3. Seismic profile across continental rise of the eastern Amundsen Sea with interpreted major sedimentary units and boundaries of a sediment drift system (modified from Uenzelmann-Neben and Gohl, 2014). CDP = common depth point.

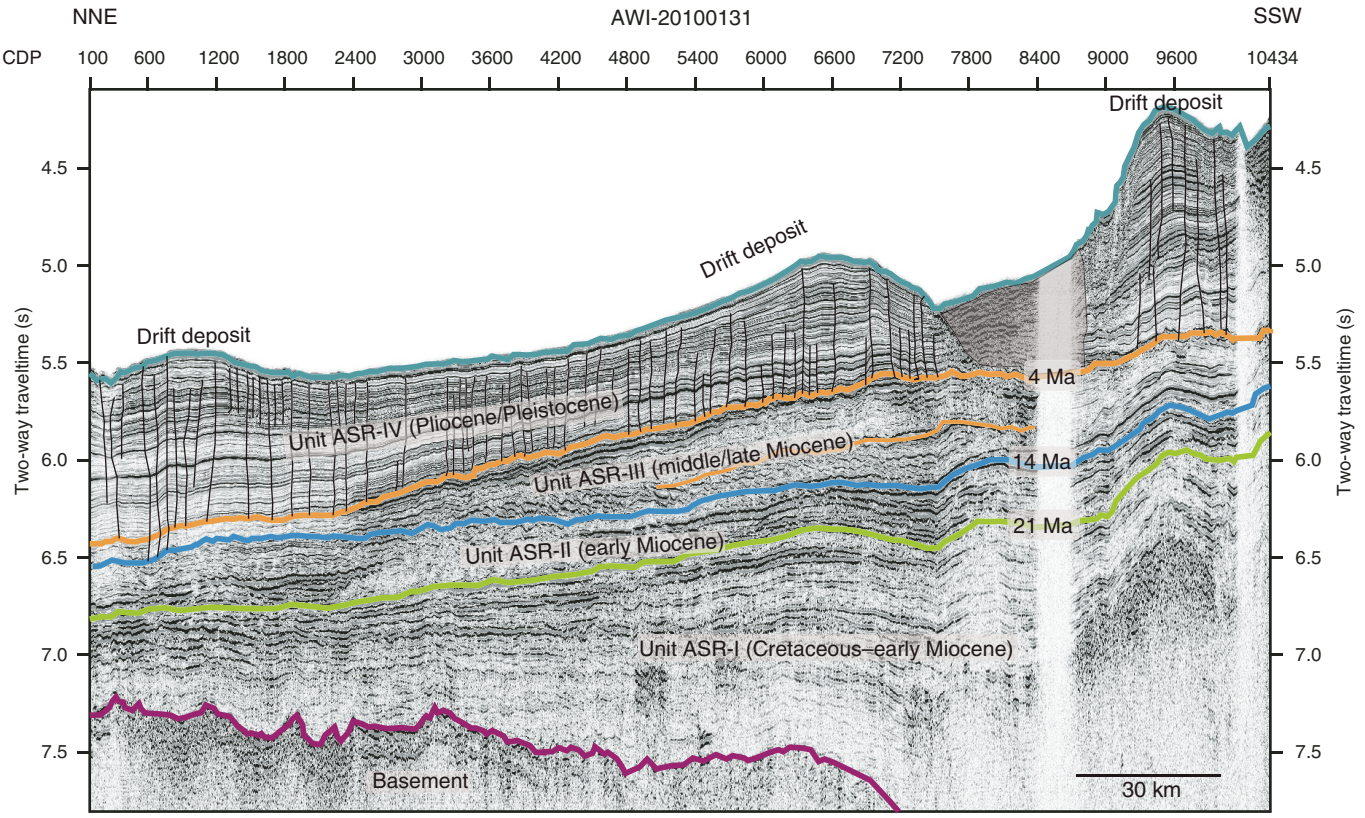

A bathymetric and structural high (Nitsche et al., 2007; Gohl et al., 2013b) separates the eastern and western Amundsen Sea continental shelves. Oceanward-dipping midshelf strata north of the outcropping basement are evident in seismic data from the Dotson-Getz Trough (Wellner et al., 2001; Graham et al., 2009; Weigelt et al., 2009; Gohl et al., 2013b) and exhibit alternating sequences of low and high reflectivity that are interpreted to be Miocene episodes of ice sheet advance and retreat. The glacial sequence stratigraphic model by Powell and Cooper (2002) proposed that glacial advances develop morainal banks consisting of unstratified diamicton, sand, and gravel that lead to a chaotic or semitransparent seismic reflection pattern. In contrast, stratified muds are deposited during a glacial retreat, which is expressed in seismic profiles as a succession of closely spaced continuous reflectors. Boundaries between the acoustic units are sharp, but without drilling, the timing of ice sheet oscillations remains unconstrained. Similar seismic facies occur on the Ross Sea and Antarctic Peninsula shelves, where drill cores confirmed that the chaotic/transparent units correspond to massive diamicton and acoustically stratified seismic facies correspond to distal glaciomarine sediments (Anderson and Bartek, 1992; Bart and Anderson, 2000; Eyles et al., 2001; Smith et al., 2010; Anderson et al., 2011).

The current seismostratigraphic model of the Amundsen Sea shelf was developed by long-distance correlation of seismic data with those of the Ross Sea shelf, which show striking similarities (Gohl et al., 2013b). Adopting the ages of the seismostratigraphic units and unconformities on the Ross Sea shelf, which are relatively well constrained by DSDP Leg 28 and ANDRILL records (e.g., De Santis et al., 1999; McKay et al., 2009), the shelf-basin formation model for the Amundsen Sea shows development from a Cretaceous synrift basin to glacially dominated strata in the Neogene and Quaternary (Gohl et al., 2013b). The seismostratigraphic record from the continental shelf is consistent with records from the Ross Sea (Bartek et al., 1991; Chow and Bart, 2003) and James Ross Basin in the northwestern Weddell Sea (Smith and Anderson, 2010), indicating a Miocene intensification of glaciation (De Santis et al., 1997) in accordance with findings from Core AND-2A (Warny et al., 2009; Passchier et al., 2011) and the Shallow Scientific Drilling on the Antarctic Continental Margin (SHALDRIL)-II drill cores (Anderson et al., 2011; Anderson and Wellner, 2011).

Apart from ice sheet dynamics inferred from the geometries and acoustic facies of seismic reflections, the ice-drainage pattern in the Amundsen Sea at the LGM and its substrate control were investigated by the analysis of sub- and proglacial bedforms visible in swath bathymetry surveys and acoustic subbottom profiler data (e.g., Larter et al., 2009). The subglacial bedforms on the shelf indicate that grounded ice expanded to the outer shelf or even the shelf edge during the recent past (Wellner et al., 2001; Lowe and Anderson, 2002; Graham et al., 2009, 2010; Jakobsson et al., 2012; Nitsche et al., 2013). Analysis of subglacial and glaciomarine sediments recovered in cores from the continental shelf confirmed an LGM age for the last WAIS advance, allowed a reconstruction of its retreat history (Lowe and Anderson, 2002; Smith et al., 2011, 2014; Kirshner et al., 2012; Hillenbrand et al., 2013; Larter et al., 2014; Klages et al., 2017), and indicated dynamically evolving drainage systems (Ehrmann et al., 2011). Recently, studies of benthic foraminiferal assemblages (Minzoni et al., 2017) and the chemical composition (i.e., stable carbon isotopes and magnesium/calcium ratios) of benthic

and planktonic foraminifer shells in ice-proximal marine sediments from the inner shelf (Hillenbrand et al., 2017) showed that variable inflow of CDW was the primary driver for grounding-line retreat along the coast of the Amundsen Sea Embayment throughout the Holocene and since the 1940s. Sedimentary sequences from the Amundsen Sea continental slope and rise spanning glacial–interglacial cycles to 1.8 Ma were investigated by multiproxy analyses to find evidence for or against a WAIS collapse during the Quaternary (Hillenbrand et al., 2002, 2009; Konfirst et al., 2012), as was previously suggested (e.g., Scherer et al., 1998; Scherer, 2003). One of these studies found a mid-Pleistocene depositional anomaly that may indicate a WAIS collapse between 621 and 478 ky ago (Hillenbrand et al., 2009). All of these studies provide a robust sedimentological framework for interpreting drill cores.

Objectives

The scientific goals and plan for this expedition are built on five hypotheses about WAIS dynamics and related paleoenvironmental and paleoclimatic conditions.

1. *Hypothesis H1: the WAIS responded to atmospheric and oceanic warming by a major retreat from the shelf or by even partial to full collapse.*

Ice sheet models hypothesize that past climate warming caused significant deglaciation of the WAIS (e.g., DeConto and Pollard, 2016). For instance, during the early middle Pliocene, Earth's climate was ~3°C warmer than at present (e.g., Haywood et al., 2009) and thus as warm as predicted for the end of this century; atmospheric pCO_2 was ~400 ppm, and other climatic boundary conditions were similar to the present (Pagani et al., 2010). The reasons for such a high atmospheric temperature during a time with modest greenhouse-gas forcing are still unknown. Results from Core AND-1B suggest repeated WAIS collapses during warm early middle Pliocene and Pleistocene interglacials (e.g., during Marine Isotope Stage [MIS] 31) (Naish et al., 2009; Pollard and DeConto, 2009; McKay et al., 2012; Villa et al., 2012). The hypothesis of WAIS collapses needs confirmation with a less ambiguous record from an outlet drainage basin exclusively affected by the WAIS. In drill cores from the Amundsen Sea margin, WAIS collapses would be recognizable by biogenic sedimentary sequences deposited during times with permanent open-water conditions and reduced supply of glaciogenic debris from the West Antarctic hinterland similar to those documented in the Core AND-1B record (Naish et al., 2009). Such sediments would contain abundant microfossils and probably tephra layers from the Marie Byrd Land volcanic province (e.g., Le Masurier and Rex, 1991; Wilch et al., 1999; Hillenbrand et al., 2008), which are essential for dating the sediments and reconstructing paleoenvironmental conditions in the region. Thus, the cores will help to answer the crucial question: did the WAIS collapse during the Neogene and Quaternary, as previously suggested, and if yes, when and under which environmental conditions?

2. *Hypothesis H2: ice-proximal records of ice sheet dynamics in the Amundsen Sea correlate with global records of ice-volume changes and proxy records for atmospheric and ocean temperatures.*

The post-LGM retreat of the WAIS from the Amundsen Sea shelf was episodic (e.g., Lowe and Anderson, 2002; Graham et al., 2009, 2010; Jakobsson et al., 2012; Larter et al., 2014). The retreat episodes were likely triggered by different processes including sea level rise, sub–ice shelf erosion by warm deepwater advection, destabilization of the ice sheet by subglacial meltwater outbursts, and grounding-line retreat into overdeepened inner-shelf basins (Jakobsson et al., 2011; Smith et al., 2011, 2014; Kirshner et al., 2012; Hillenbrand et al., 2013, 2017). These observations raise questions concerning the linkage between climate and glaciological forcing in regulating WAIS deglaciation. Throughout the Cenozoic era, unexplained discrepancies are observed between Earth's temperature and global ice volume reconstructed from proxies in deep-sea sediments, climate models, sea level estimates, and ice cores for the last 800 ky. Reexamination of previously studied cores highlights ongoing uncertainty about the timing and extent of early ice sheet growth (Carter et al., 2017). The results of the Core AND-1B record (Naish et al., 2009) and Integrated Ocean Drilling Program Expedition 318 to the Wilkes Land margin (Cook et al., 2013) reignited the debate as to whether the Antarctic ice sheets underwent major collapses during Pliocene interglacials. Such collapses are neither directly recognizable from oxygen isotope proxies at far-field sites nor confirmed by the apparently persistent glaciation of the Antarctic Peninsula since the latest Miocene (Smellie et al., 2009). Furthermore, evidence of repeated Pliocene ice sheet advances across the shelf are observed in seismic profiles all along the Antarctic margin (e.g., Larter et al., 1997; Nitsche et al., 1997; Bart and Anderson, 2000; Smith and Anderson, 2010; Bart, 2001). Indeed, results from SHALDRIL cores and other data from the eastern Antarctic Peninsula shelf indicate gradual cooling and an associated decline in vegetation over the past 37 My culminating in early Pliocene ice sheet expansion onto the continental shelf (Anderson et al., 2011). Results from Leg 178 cores from the western Antarctic Peninsula shelf and rise are consistent with repeated ice sheet advances throughout the Pliocene (Eyles et al., 2001; Hillenbrand and Ehrmann, 2005; Hepp et al., 2006; Bart, 2001) but also indicate significant oceanic warming during Pliocene interglacials (Hillenbrand and Cortese, 2006; Escutia et al., 2009; Hepp et al., 2009; Bart and Iwai, 2012). Expedition 379 drill sites will help us decipher whether the WAIS responded directly to the orbitally paced climatic cycles of the Pliocene and Quaternary or varied at periods determined by its internal dynamics, as findings from Leg 178 suggest for the Antarctic Peninsula Ice Sheet (Barker and Camerlenghi, 2002). Similar to cores from the Ross Sea shelf (McKay et al., 2009), Leg 178 cores from the Antarctic Peninsula shelf are incomplete because of glacial erosional unconformities (Eyles et al., 2001). During Expedition 379, cores were drilled from deep-sea drifts on the continental rise offshore from the Amundsen Sea Embayment to obtain complete sedimentary sequences. Similar drift sediments drilled on the western Antarctic Peninsula continental rise during Leg 178 provided excellent archives of Neogene to Quaternary ice sheet dynamics and paleoenvironmental changes (e.g., Hillenbrand and Ehrmann, 2005; Cowan et al., 2008; Hepp et al., 2006, 2009; Escutia et al., 2009; Bart and Iwai, 2012). A comparable potential has already been demonstrated for Pleistocene drift sediments recovered from the Amundsen Sea continental rise (Hillenbrand et al., 2009).

3. *Hypothesis H3: the stability of marine-based WAIS margins is and has been controlled by warm deepwater incursions onto the shelf.*

In model experiments, incursions of relatively warm CDW onto the West Antarctic continental shelf have been implicated in regulating WAIS behavior on orbital and suborbital timescales (Pollard and De Conto, 2009; Dutrieux et al., 2014). Therefore, records of past CDW upwelling are urgently needed to understand the rela-

tionship between WAIS dynamics and ocean circulation. Generating proxy records of past CDW incursions from marine sediment cores is still a challenge but was recently demonstrated to be possible in sediments from the Amundsen Sea Embayment shelf (Hillenbrand et al., 2017; Minzoni et al., 2017). With recent observations of present CDW advection predominantly through the paleo–ice stream troughs of the Amundsen Sea (e.g., Arneborg et al., 2012), drill cores from the continental shelf would provide sample material suitable for applying benthic foraminifer–based and other proxies to reconstruct past CDW upwelling onto the shelf and its effect on WAIS dynamics. However, proxy investigations on sediment records from the continental rise will also provide insights on deepwater circulation and CDW advection toward the Amundsen Sea shelf.

4. *Hypothesis H4: major WAIS advances onto the middle and outer shelf have occurred since the middle Miocene.*

Seismic data revealed progradational and aggradational deposition on the outer shelf and slope of the Amundsen Sea, probably since the mid-Miocene (e.g., Nitsche et al., 1997, 2000; Hochmuth and Gohl, 2013; Gohl et al., 2013b). Numerous unconformities within strata on the shelf document frequent advance and retreat of grounded ice from the late Miocene until the Pliocene/Pleistocene, according to the stratigraphic age model by Gohl et al. (2013b). The preservation of buried grounding-zone wedges in the Pliocene–Pleistocene sequence on the outer Amundsen Sea shelf is consistent with the prolonged continuous accumulation of marine and glaciomarine sediments in an open-marine setting, probably during a long interglacial period with a significantly reduced WAIS, as observed on the Ross Sea shelf during the early Pliocene. However, the models of grounded-ice advance and retreat across the Amundsen Sea shelf are based on long-distance correlations of seismic facies and characteristics, which are tested by core data to constrain past WAIS extent.

5. *Hypothesis H5: the first WAIS advance onto the inner Amundsen Sea continental shelf occurred during the Oligocene and was related to the uplift of Marie Byrd Land.*

The onset of major glaciation in West Antarctica is still not dated because of sparse drill cores. Records of ice-rafted debris (IRD) suggest that glaciers must have reached the coast of the Ross Sea in the early to mid-Oligocene (Miller et al., 2008). Ice sheet models (e.g., DeConto and Pollard, 2003) reconstructed an early WAIS nucleus in the mountain chain extending from elevated Marie Byrd Land over the Ellsworth Mountains to the southern Antarctic Peninsula. The exhumation and erosion history of Marie Byrd Land and especially the Marie Byrd Land dome is essential for the interrelations between ice sheet and lithosphere dynamics (e.g., Rocchi et al., 2006; Wilson and Luyendyk, 2009; Wilson et al., 2012, 2013; Spiegel et al., 2016) because (1) exhumation and erosion change topography, which in turn influences glacier movements by slope steepness; (2) exhumation is often associated with surface uplift, and high altitude favors formation of glaciers; and (3) glaciation changes erosion rates and, because of isostatic adjustment, exhumation rates. This relationship can be investigated using detailed provenance and thermochronological analyses of IRD from Neogene drill samples and existing rock samples from the hinterland.

Operations plan/drilling strategy

The primary aim of our drilling campaign was to obtain core and log data from seaward-dipping strata along a transect from the Paleogene sequences close to the boundary with bedrock on the inner shelf to the Pliocene to Pleistocene sequences on the outer shelf and continuing onto the continental rise for continuous high-resolution records. Because sea ice conditions during the drilling expedition were unsuitable for accessing either the priority sites in Pine Island Trough or the transect targeting strata of comparable age and cross-shelf position in the Dotson-Getz Trough, we drilled our third-tier priority sites on the continental rise. The sites we drilled during Expedition 379 were added to the proposal following the record austral summer sea ice extent in 2017/2018. The two sites (U1532 and U1533) were not lower in priority than other rise sites; instead, they were added to the proposal in 2018, when sites were no longer required to be on a crossing seismic line. This change provided an opportunity for alternates even farther north and thus farther from likely sea ice cover than the originally proposed sites. Additional modifications in 2018 to our original proposal included approval of "ribbons" along the seismic line that allowed holes to be drilled in a range of positions and for maximum flexibility in severe ice conditions.

Our plan was to core two holes at each drill site using the advanced piston corer (APC), half-length APC (HLAPC), and extended core barrel (XCB) systems in the first hole and the rotary core barrel (RCB) system in the second hole and then collect log data in the deeper RCB hole. In reality, each of our two drill sites included far more holes than intended. Site U1532 includes seven holes, and Site U1533 has four holes. No holes were terminated by reaching target depths; we terminated the first 10 holes because of approaching icebergs, and we had to abandon the final hole because of an emergency medical evacuation.

The coring strategy at each site generally followed the operational plans; however, it was spread out over multiple holes. When we were forced to leave a hole, we drilled a new hole without coring through the upper section, and then coring resumed with some overlap. We initiated new holes following a standard offset of 20 m except when ice conditions would not allow a new hole close to the original site and other positions along the permitted ribbon were open. Thus, the holes at each site are more spread out than those of many other IODP expeditions.

Although downhole logging was planned for each site, no downhole log data were collected during Expedition 379 because of the premature termination of each hole.

Site summaries

Site U1532

Background

Site U1532 (Proposed Site ASRE-08A) is located on the western upper flank of a large sediment drift (Resolution Drift) on the continental rise, 270 km north of the Amundsen Sea Embayment shelf edge (Figures **F1**, **F4**). This drill site was chosen as the first Expedition 379 site upon arriving in the Amundsen Sea because the sea ice distribution did not allow drilling at any of the other primary or alternate sites at that time. The Resolution Drift belongs to a system of five parallel sediment drifts on this rise that are characterized by gentle western and steep eastern flanks. Sediment drifts are commonly formed by deposition of suspended sediments transported by ocean-bottom contour currents. Deep-sea channels that originate at the foot of the continental slope and reach far into the abyssal plain separate the sediment drifts in the Amundsen Sea. Sediment is transported downslope through these channels by turbidity currents, slumps, and other gravity-driven processes that

Figure F4. Site U1532 on the northwestern segment of Seismic Line AWI-20100130 that crosses the Resolution Drift. Seismic horizons at the bases of the Pleistocene and Pliocene were preliminarily identified from the core records. Estimated age of the horizon at the base of Unit ASR-II is from Uenzelmann-Neben and Gohl (2014).

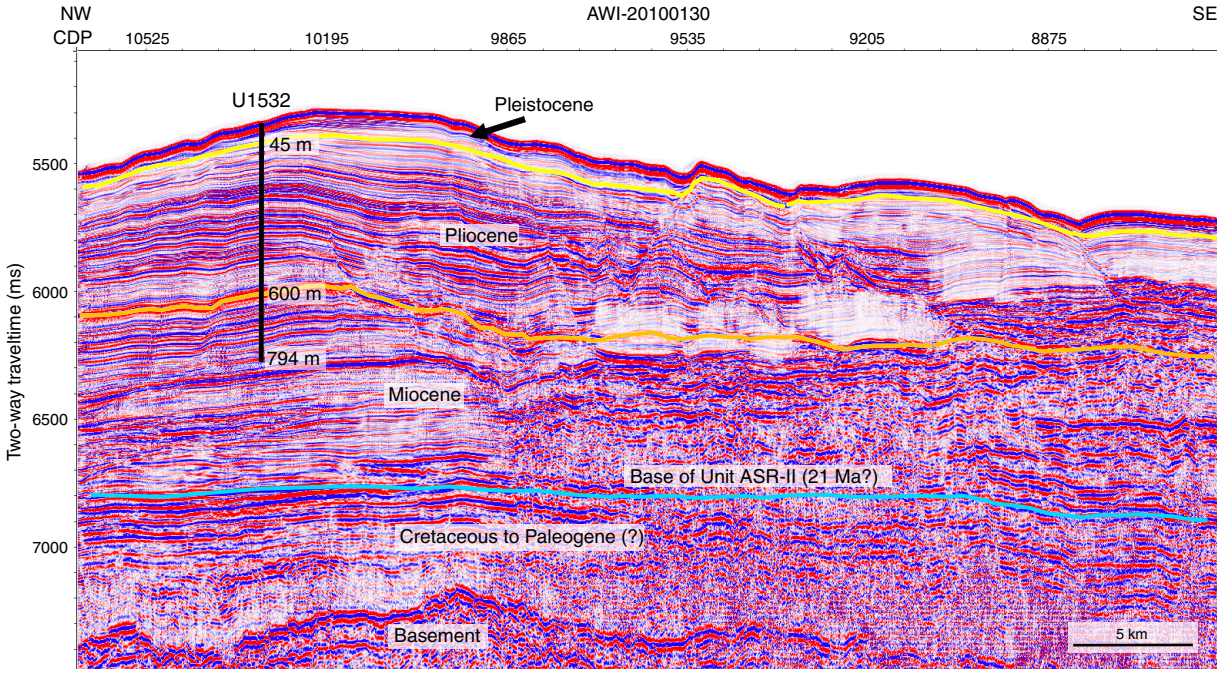

supply a large portion of the detritus deposited on the drifts (Nitsche et al., 2000; Dowdeswell et al., 2006). Sedimentation rates of drift deposits along the Antarctic margin are extremely high, which makes them high-priority drill targets to obtain continuous paleoceanographic and paleo–ice sheet records of high temporal resolution (e.g., Barker and Camerlenghi, 2002; Uenzelmann-Neben and Gohl, 2012). Stratigraphic interpretations of seismic lines across the sediment drifts of the Amundsen Sea (e.g., Nitsche et al., 2000; Scheuer et al., 2006b; Uenzelmann-Neben and Gohl, 2012, 2014) are, so far, only inferred from long-distance correlation with drift deposits on the Antarctic Peninsula rise, for which age constraints from drill core exist (Leg 178; e.g., Acton et al., 2002). However, the interpretations suggest equally high sedimentation rates for the Pleistocene, Pliocene, and upper Miocene.

Seven holes (U1532A–U1532G) were drilled in 3962 m water depth (Figure **F5**). The deepest hole (U1532G) was drilled to 794 m. Overall core recovery was 90%. Although sea ice was not a problem for the R/V *JOIDES Resolution* at this site, icebergs of various sizes, from large tabular icebergs to smaller fragments and growlers, frequently approached the ship and were the primary reason for the large number of holes. Holes U1532E and U1532F were nothing more than unsuccessful attempts to start coring at depth before being forced to avoid another iceberg approach.

Lithostratigraphy

Deposits at Site U1532 include silty clay(stone) with dispersed sand and gravel and variable biogenic content recovered from five holes down to 787.4 m. Six lithofacies were identified based on visual characteristics of the sediments combined with information from smear slides and thin sections. Whole-core X-radiographs aided in observations of sedimentary structures, clast occurrence, and drilling disturbance. The dominant lithofacies assemblages are planar thinly laminated silty clay(stone) with occasional occurrences of massive and bioturbated silty clay(stone) typically <1.5 m thick. We observed dispersed sand grains, granules, and occasional pebbles throughout the assemblages, but they appear mainly concentrated within the massive and bioturbated facies. Minor lithofacies include foraminifer-rich and biosilica-rich mud to ooze.

Figure F5. Distribution of Holes U1532A–U1532G. See Figure F1 for regional location map.

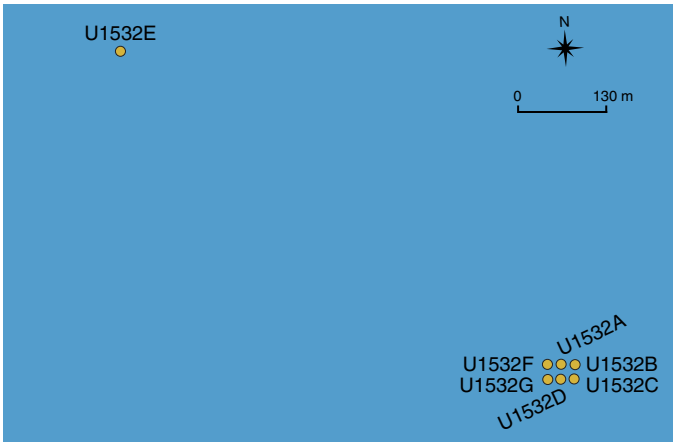

We identified one lithostratigraphic unit with three subunits based on changes in facies assemblages: Lithostratigraphic Subunits IA (0–92.6 m; recent–Pliocene), IB (92.6–400.6 m; Pliocene), and IC (401.0–787.4 m; Pliocene–Miocene). The sediments are unconsolidated in the upper 150 m and become increasingly more consolidated below this depth. Intervals of carbonate-cemented laminae and very thin beds of coarse siltstone and sandstone are present below 400 m.

Biostratigraphy

In the upper part of the section recovered at Site U1532 (i.e., Subunit IA; 0–92.6 m), sufficient microfossils for biostratigraphic age assignment were only present in the upper ~10 m, providing an age of middle Pleistocene to recent (0–0.6 Ma). Sediments between ~10 and ~90 m were nearly barren of datable microfossils, whereas diatoms and radiolarians from ~92 to 156 m provided biostratigraphic ages of mid- to late Pliocene (3.2–3.8 Ma), and sediments from ~156 to 224 m were assigned an early Pliocene age of 3.8–4.4 Ma. The absence of microfossils or only trace occurrences of highly fragmented and recrystallized siliceous microfossils in samples below ~224 m in Hole U1532G precluded shipboard biostratigraphic age determination at most levels. Exceptions include short intervals with poorly preserved but identifiable diatoms between ~224 and 332 m (early Pliocene; younger than 4.7 Ma) and between ~332 and 510 m (early Pliocene to near the Miocene/Pliocene boundary; younger than 5.5 Ma).

Some light green, bioturbated biosilica-rich intervals coincide with higher concentrations of coarse sand and gravel, which are inferred to be IRD. Some stratigraphic intervals contain little or no identifiable diatom debris despite possessing low magnetic susceptibility and gamma ray attenuation (GRA) bulk density and a greenish color, which are characteristics typical of diatomaceous units. The lack of diatoms in these intervals is inferred to reflect, at least in part, diagenetic loss of diatoms and other siliceous microfossils. Organic microfossils occur in relatively low abundance throughout the Site U1532 sequence. A possibly in situ dinoflagellate cyst (dinocyst) assemblage of very low diversity and low abundance is present throughout the section, but this assemblage is more persistent and thus very likely to be in situ below 591.77 m. Calcareous microfossils including foraminifers, calcareous nannofossils, and ostracods generally occur in the absence of biosiliceous material in thin intervals in the Pleistocene section.

Paleomagnetism

The interpreted magnetic polarity at Site U1532 was correlated with the Gradstein et al. (2012) geological timescale (GTS2012). The resulting key paleomagnetic data were then integrated with biostratigraphic data to produce an age model.

For Hole U1532A, we obtained robust shipboard magnetostratigraphy that consists of four normal and four reversed polarity intervals. The Brunhes–Matuyama polarity transition (0.781 Ma), the termination and beginning of the Olduvai Subchron (1.778 and 1.945 Ma, respectively), the Matuyama–Gauss polarity transition (2.581 Ma), the termination and beginning of the Kaena Subchron (C2An.1r; 3.032 and 3.116 Ma, respectively), and the termination and beginning of the Mammoth Subchron (C2An.2r; 3.207 and 3.330 Ma, respectively) were identified. Paleomagnetic measurements for Hole U1532B identified the beginning of the Mammoth Subchron (C2An.2r; 3.330 Ma) and the Gauss–Gilbert polarity transition (3.596 Ma). Paleomagnetic measurements for Hole U1532C identified the termination of the Nunivak Subchron (C3n.2n; 4.493 Ma) but no clear Cochiti Subchron (C3n.1n; 4.187–4.300 Ma). Natural remanent magnetization (NRM) measurements for Hole U1532G identified the beginning of the Nunivak Subchron (C3n.2n; 4.631 Ma), the termination and beginning of the Sidufjall Subchron (C3n.3n; 4.799 and 4.896 Ma, respectively), and the termination and beginning of the Thvera Subchron (C3n.4n; 4.997 and 5.235 Ma, respectively). Reversed magnetic polarity continues downcore to the bottom of Hole U1532G. The beginning of Chron C3r (6.033 Ma) was not observed. Therefore, the oldest sediments recovered at Site U1532 are presumably of late Miocene age.

Geochemistry

At Site U1532, 65 interstitial water samples were collected and measured for salinity, alkalinity, pH, major ions (sodium [Na], potassium [K], calcium [Ca], magnesium [Mg], chloride [Cl], and sulfate [SO_4)]), nutrients (ammonium [NH_4] and phosphate [PO_4]), silica ($H_4Si[OH]_4$), and trace elements (strontium [Sr], lithium [Li], iron [Fe], manganese [Mn], boron [B], and barium [Ba]). Drilling fluid contamination was detected in a few interstitial water samples taken from XCB cores. Higher abundances of perfluorocarbon tracer (PFT) in these samples are in line with this observation. The sulfate downhole profile shows a sharp linear decrease from ~28 mM near the surface to ~2.3 mM at ~664 m; however, sulfate concentration did not reach zero at this site, indicating a low sulfate reduction rate. The Ca and Sr profiles show an overall increase, whereas the K and Mg profiles display the reverse trend. Silica concentration is relatively high from 8.5 to 238 m, coinciding with intervals where a higher abundance of diatoms was observed. Diagenesis of diatoms through reaction with the interstitial water likely resulted in higher silica concentration.

Calcium carbonate ($CaCO_3$) content is low in the sediments of Lithostratigraphic Subunit IA; discrete maxima in $CaCO_3$ observed in the upper section of Subunit IA are linked to layers rich in calcareous foraminifer tests. Subunit IB is characterized by a general increase in $CaCO_3$ downhole. Total organic carbon (TOC) content is generally low at Site U1532 but displays a small stepwise increase from Subunit IA to Subunit IC. Total nitrogen content is low throughout all subunits. Total sulfur (TS) content decreases throughout Subunit IA and generally remains low throughout Subunit IB. TS displays a downhole increase in the uppermost section of Subunit IC (to ~533 m). Below ~533 m, TS declines again and then shifts to low values below ~670 m. This shift in TS content is associated with a near depletion of interstitial water sulfate concentrations, which may limit sulfate reduction and the formation of iron sulfides at greater depth.

Headspace gas samples to monitor for the presence and abundance of C_1–C_3 hydrocarbons indicate that methane occurs in only very low concentrations throughout the upper ~650 m. At ~667 m, methane concentration increases rapidly, exceeding 5000 ppmv below ~713 m and reaching a maximum of 9517 ppmv at ~771 m. The increase of methane at ~667 m coincides with a pronounced minimum in sulfate, suggesting that methane may be of biogenic origin at Site U1532.

Physical properties

Collected physical property data include magnetic susceptibility, natural gamma radiation (NGR), GRA bulk density, discrete moisture and density (MAD), *P*-wave velocity, thermal conductivity, in situ formation temperature (advanced piston corer temperature tool [APCT-3]), and spectral color reflectance. Whole-round magnetic susceptibility trends follow those observed in GRA bulk density and NGR, likely indicating changes in terrigenous sediment content. Magnetic susceptibility data were used as a primary tool for correlating cores from adjacent holes. Measured whole-round magnetic susceptibility ranges between 8×10^{-5} and 241×10^{-5} SI. Average magnetic susceptibility values increase downhole from ~80 $\times 10^{-5}$ to ~120 $\times 10^{-5}$ SI at ~93 m, which corresponds to the Lithostratigraphic Subunit IA/IB boundary. Measured NGR ranges between 19 and 112 counts/s with an overall average of 69 counts/s. Average NGR values increase downhole from ~43 counts/s at the mudline to ~75 counts/s at ~93 m, which corresponds to the Subunit IA/IB boundary. Below ~93 m, magnetic susceptibility and

NGR vary cyclically between ~15 × 10^{-5} and ~100 × 10^{-5} SI and ~30 and 80 counts/s, respectively. In the upper 65 m, bulk density increases downhole from ~1.5 to ~1.8 g/cm^3, followed by a more gradual increase to ~2.1 g/cm^3, reflecting increasing compaction. Intervals of lower magnetic susceptibility, NGR, and GRA bulk density correspond to greenish gray intervals in Subunits IB and IC. Sediment porosity decreases downhole from 77% at the seafloor to 58% at 30 m and decreases further with depth to 33% at the bottom of Hole U1532G, reflecting the downward compaction trend of marine sediments. *P*-wave velocity increases with depth from ~1460 m/s at the seafloor to ~2090 m/s at the base of Hole U1532G. No major changes in *P*-wave velocity were observed across the lithostratigraphic subunit boundaries. Thermal conductivity increases with depth from ~1 W/(m·K) at the seafloor to ~1.8 W/(m·K) at ~390 m, corresponding to a downhole increase in dry bulk density and decrease in porosity due to compaction. Formation temperature measurements from 34 to 150 m in Hole U1532A were used to estimate a geothermal gradient of ~54°C/km.

Site U1533

Background

Site U1533 (Proposed Site ASRE-09A) is located 62 km west-southwest of Site U1532 on the westernmost lower flank of the Resolution Drift, the same sediment drift as Site U1532, on the continental rise of the Amundsen Sea (Figures **F1**, **F6**). This lower flank is bound by a north–south oriented deep-sea channel west of Site U1533 (Uenzelmann-Neben and Gohl, 2012). The channel is likely the path of sediment transported downslope from the shelf by turbidity currents and sediment gravity flows and, as such, is likely the major source of terrigenous sediment to the drill site (e.g., Dowdeswell et al., 2006). Bottom currents transported clay- and silt-sized particles before they deposited them to form a drift (e.g., Nitsche et al., 2000). A robust horizon correlation from Site U1532 performed along three connected seismic lines indicates that sedimentary sequences of the same age are more condensed at Site U1533.

Four holes (U1533A–U1533D) were drilled at Site U1533 in water depths between 4179 and 4184 m (Figure **F7**). The deepest penetration (Hole U1533B) reached 383 m with an overall core recovery of 70%. As at Site U1532, frequent approaches of icebergs of various sizes were the primary reason for the large number of holes.

Lithostratigraphy

Sediments recovered at Site U1533 consist mainly of silty clay(stone) with varying biogenic content and amounts of bioturbation as well as rare occurrences of diamict and conglomerate. Thin sand(stone) and silt(stone) beds and laminae occur throughout, and intervals of carbonate cementation and volcaniclastic material were also observed. The recovered sediments are categorized into seven lithofacies based on visual characteristics and lithologic information supported by smear slide observations. The drilled sequence is divided into Lithostratigraphic Subunits IA (0–54.9 m) and IB (54.9–381.2 m) based on changes in facies assemblages. Whole-core X-radiographs were used to aid in the identification of sedimentary structures, clast occurrence, and drilling disturbance. Site U1533 is dominated by deposition of fine-grained sediments interpreted to be initially supplied by sediment gravity flows from the continental shelf and subsequently reworked by contour currents. Silt and sand beds are interpreted to have been deposited by overspill of turbidity currents from the submarine channel. Additionally, a significant amount of biosiliceous material in the sediments is supplied from the overlying surface waters.

The association of facies in Lithostratigraphic Subunit IA predominantly reflects the interplay of downslope and contouritic sediment supply that also includes input of more pelagic sediment during phases of seasonally open marine conditions. The amount of biogenic material is generally high throughout Subunit IA, suggest-

Figure F6. Site U1533 on Seismic Line TH86003B (Yamaguchi et al., 1988) at the lowermost western flank of the Resolution Drift. Seismic horizons at the bases of the Pleistocene and Pliocene were preliminarily identified from the core records. Estimated age of the horizon at the base of Unit ASR-II is from Uenzelmann-Neben and Gohl (2012).

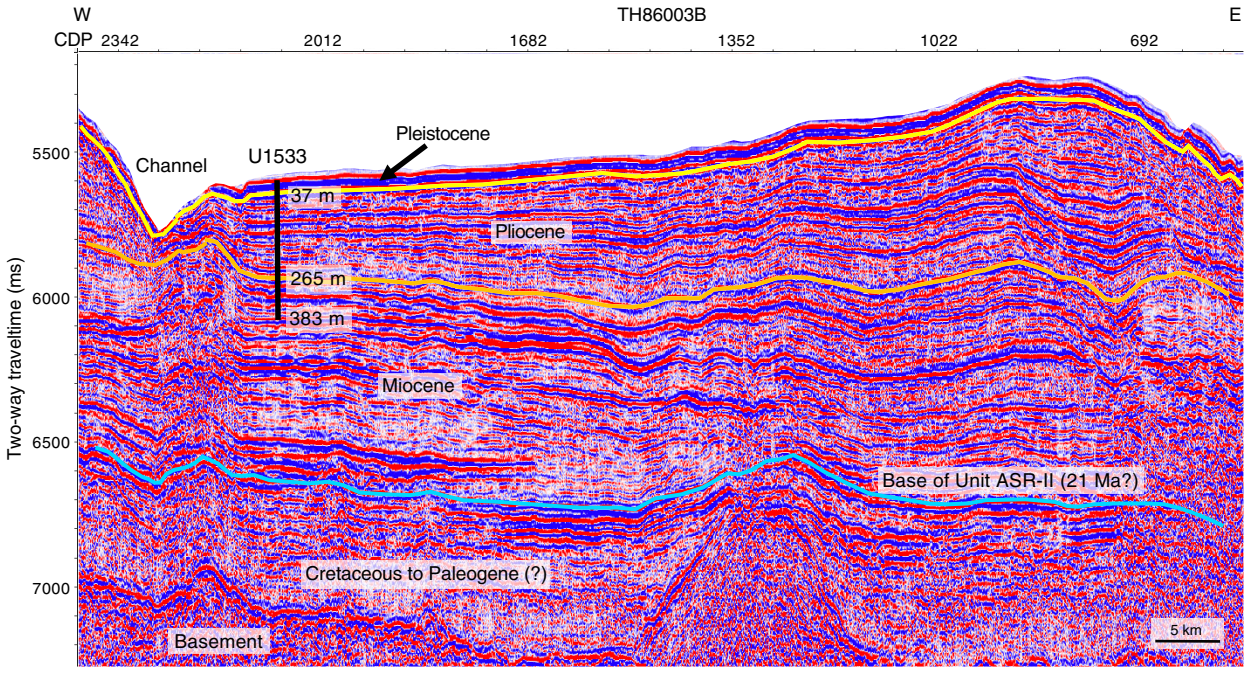

Figure F7. Distribution of Holes U1533A–U1533D. See Figure F1 for regional location map.

ing sustained periods of relatively high marine productivity. Deposits related to downslope transport are present throughout the sedimentary record at Site U1533. In Subunits IA and IB, coarse-grained beds indicate that overspill deposition probably originated from downslope transport through the adjacent deep-sea channel. Subunit IB has generally higher amounts of visible clasts and pebbles than Subunit IA. Dispersed granules and pebbles, clast nests, and discontinuous bands of coarse sand and granules in Subunits IA and IB are inferred to indicate persistent but likely low-intensity ice rafting, and there is a higher abundance of this IRD within diatom ooze intervals.

Biostratigraphy

In contrast with Site U1532, which contains significant intervals that are barren of microfossils, the majority of Site U1533 samples from the mudline to the lowermost sediments contain siliceous microfossils with variable preservation and organic-walled microfossils, dominantly reworked terrestrial palynomorphs. Preservation and abundance of microfossils are highly variable, including some barren intervals noted in the lowermost Pleistocene–uppermost Pliocene and lower Pliocene sections. A similar general pattern of alternating gray-beige to brownish sediments (Lithostratigraphic Subunit IA) and gray-beige to greenish sediments (Subunit IB) at Site U1532 was commonly observed at Site U1533. At Site U1533, they consisted of gray, laminated, microfossil-poor, mostly terrigenous mudstones punctuated by thinner brownish to greenish, bioturbated, variably biosilica-bearing intervals, some with sand- to pebble-sized material interpreted to be IRD. Despite the proximity to Site U1532, the brownish and greenish bioturbated units of Site U1533 have a significantly higher overall concentration of biosiliceous material.

The diatom assemblages are heavily dominated by pelagic forms with little evidence of sea ice or neritic environments. We speculate that the difference between Sites U1532 and U1533, with respect to Pleistocene biosilica accumulation and preservation, is due to a lower terrigenous flux and higher deposition of pelagic diatoms advected from farther offshore rather than a difference in local diatom production between the surface water at the sites.

The upper ~40 m of Site U1533 spans the recent to Pleistocene and contains variable concentrations of diatoms, radiolarians, and foraminifers; rare marine and reworked terrestrial palynomorphs; and very rare calcareous nannofossils. Diatoms and radiolarians are present in most samples examined from this interval. Foraminifers are present only in a few intervals in the upper ~10 m of the sequence.

Pleistocene to upper Miocene sediments recovered from Hole U1533B are dated primarily by diatoms and radiolarians. Both groups are documented with variable abundance from the top to the base of Hole U1533B. Samples from the lowermost cores generally contain common to abundant diatoms, although the frustules are highly fragmented. Diatoms and radiolarians provide a latest Miocene age (6.2–6.7 Ma) for the lowermost sediments recovered from Hole U1533B. Combined with magnetostratigraphic constraints, the deepest sediments recovered in Hole U1533B are ~6.4–6.75 Ma. In situ foraminifers and calcareous nannofossils were not observed in the Pliocene sediments in Hole U1533B, whereas rare to common marine and reworked terrestrial palynomorphs are present throughout.

Paleomagnetism

For Hole U1533A, demagnetization of NRM at 20 mT identifies the Brunhes–Matuyama transition (0.781 Ma), the termination and beginning of the Jaramillo Subchron (C1r.1n; 0.988 and 1.072 Ma, respectively), and the termination and beginning of the Cobb Mountain Subchron (C1r.2n; 1.173 and 1.185 Ma, respectively).

The magnetostratigraphy is more complex for Hole U1533B than for Hole U1533A because of reduced core recovery and drilling disturbance of some intervals. The shipboard interpretation identifies the beginning of the Olduvai Subchron (C2n; 1.945 Ma), the termination and beginning of Subchron C2An.1n (2.581 and 3.032 Ma, respectively), the termination and beginning of Subchron C2An.3n (3.330 and 3.596 Ma, respectively), the termination and beginning of the Cochiti Subchron (C3n.1n; 4.187 and 4.300 Ma, respectively), and the termination and beginning of the Nunivak Subchron (C3n.2n; 4.493 and 4.631 Ma, respectively). Subchron C2An.2n (3.116–3.207 Ma) might be present in a very condensed form in Core 379-U1533B-5H at ~58 m. Farther downhole, paleomagnetic measurements reveal the termination and beginning of the Sidufjall Subchron (C3n.3n; 4.799 and 4.896 Ma, respectively) and the termination and beginning of the Thvera Subchron (C3n.4n; 4.997 and 5.235 Ma, respectively). Below an interval without core recovery, the deepest cores with significant recovery, 39R and 43R, are of mainly normal polarity, suggesting a basal age for Hole U1533B between the termination of Subchron C3An.1n (6.033 Ma) and the beginning of Subchron C3An.2n (6.733 Ma). Oscillating normal and reversed polarity at the bottom of Hole U1533B provides no clear evidence that Subchron C3Ar was recovered.

For Hole U1533C, no magnetic polarity reversal was recorded, suggesting that the recovered sediments are younger than the Brunhes–Matuyama transition (0.781 Ma).

For Hole U1533D, paleomagnetic measurements identified the Brunhes–Matuyama transition (0.781 Ma), the termination and beginning of the Jaramillo Subchron (C1r.1n; 0.988 and 1.072 Ma, respectively), the termination and beginning of the Cobb Mountain Subchron (C1r.2n; 1.173 and 1.186 Ma, respectively), and the termination and beginning of the Olduvai Subchron (C2n; 1.778 and 1.945 Ma, respectively).

Chronostratigraphy

By combining biostratigraphy and magnetostratigraphy, the interval above ~37 m is assigned a recent to Pleistocene age, the interval from ~37 to 265 m is assigned a Pliocene age, and the interval from ~265 to 383 m (base of recovery at Site U1533) is assigned a latest Miocene age. The combined data indicate a 6.4–6.75 Ma age for the base of Hole U1533B at 381.23 m.

Geochemistry

Interstitial water salinity at Site U1533 is constant at 35 from the seafloor to ~235 m and is slightly lower (33 to ~34) from 255 to 375 m. Cl concentration ranges between 557 and 596 mM. The elevated

Cl concentrations in the deeper section of Site U1533 could be due to hydration reactions during clay formation. Na concentration ranges between 440 and 483 mM throughout the section. Below ~17 m, sulfate decreases continuously with depth and reaches its minimum (~1.6 mM) at 375 m. Interstitial water alkalinity increases linearly with depth from 1.5 m to a maximum (~10.5 mM) at ~185 m, which is the opposite trend to that of sulfate. Below ~185 m, alkalinity slightly decreases with depth to 375 m.

Sr concentration shows an overall increase from 82 µM at 1.5 m to 196 µM at 375 m, reaching maximum values ~2.5 times higher than the measured modern seawater value (82 µM). The higher Sr concentration indicates either higher fluid-rock reaction with volcaniclastic material or dissolution of carbonates.

Methane concentration is ~4 ppmv, which is close to the instrumental background signal, in Hole U1533A and most of Hole U1533B. At 325.60 m, methane concentration abruptly increases downhole to a peak of 6373 ppmv at 375.02 m. No hydrocarbons other than methane were detected at Site U1533. Increased methane was found only at the base of Lithostratigraphic Subunit IB, where the lowest sulfate concentration was observed. Together with the absence of higher hydrocarbons, this may suggest a biological source of methane at Site U1533.

Total carbon content varies between 0.02 and 0.5 wt% and increases with depth. $CaCO_3$ is low at Site U1533 and ranges between 0.02 and 2.54 wt%. TOC content varies between 0.01 and 0.41 wt% and is similar to the total carbon record in terms of trends and abundances, indicating that organic carbon constitutes most of the total carbon pool.

Samples for contamination testing were collected from the exterior and center of freshly exposed core sections or whole-round samples. PFTs were present in variable concentrations in samples taken from most APC core exteriors because of the direct exposure of the core surface to circulating drilling fluids. However, tracer concentrations are approximately four orders of magnitude lower in these samples than the target concentrations of tracers in the drilling fluid. Tracers were below detection in the interior of most APC and HLAPC cores. The absence of tracers in the central parts of most APC/HLAPC cores and their generally low presence in core exteriors suggest low overall contamination. XCB cores generally show low contamination in both the interior and exterior samples, but in contrast to APC/HLAPC cores, contamination was consistently present in the center of the cores. The sampled RCB cores generally showed higher levels of tracer contamination than APC/HLAPC and XCB cores.

Physical properties

Collected physical property data include magnetic susceptibility, NGR, GRA bulk density, MAD, *P*-wave velocity, thermal conductivity, and spectral color reflectance. Whole-round magnetic susceptibility trends follow those observed in GRA bulk density and NGR, likely indicating changes in terrigenous sediment content. Magnetic susceptibility data were used as a primary tool for correlating cores from adjacent holes to create a shipboard splice for the uppermost ~44 m of the site. Measured whole-round magnetic susceptibility ranges between 5×10^{-5} and 805×10^{-5} SI. Average magnetic susceptibility values increase downhole from ~50×10^{-5} to ~100×10^{-5} SI at 55 m, which corresponds to the Lithostratigraphic Subunit IA/IB boundary. Measured NGR ranges between 13 and 235 counts/s with an overall average of 56 counts/s. Average NGR values increase downhole from ~20 counts/s at the mudline to ~60 counts/s at 55 m, which corresponds to the Subunit IA/IB boundary. Below ~55 m, magnetic susceptibility and NGR vary cyclically between ~10×10^{-5} and ~130×10^{-5} SI and ~30 and ~75 counts/s, respectively. The GRA bulk density record shows a sharp downhole increase from ~1.3 to ~1.8 g/cm^3 in the uppermost 55 m that corresponds to Subunit IA. Below this depth, GRA bulk density exhibits several stepwise changes. The overall increase in GRA bulk density with depth at this site reflects the increasing compaction of sediment with depth. Smaller scale variability indicates changes in sediment lithology and correlates well with NGR and magnetic susceptibility variability. In the upper ~15 m of Holes U1533A, U1533C and U1533D, magnetic susceptibility, NGR, and GRA bulk density exhibit a "sawtooth" pattern with a sharp increase in overall value followed by a more gradual decline downcore.

Sediment porosity decreases downhole from 86% at the seafloor to 65% at ~30 m and decreases further with depth to 45% at the bottom of Hole U1533B, reflecting the downward compaction trend of marine sediments. *P*-wave velocity increases from ~1480 m/s at the seafloor to an average velocity of ~1760 m/s at the termination of Hole U1533B at 380 m. Below ~55 m in Lithostratigraphic Subunit IB, *P*-wave velocity varies with sediment texture. Thermal conductivity increases with depth from ~0.7 W/(m·K) at the seafloor to ~1.4 W/(m·K) at ~375 m and corresponds to a downhole increase in dry bulk density and decrease in porosity from compaction.

Preliminary scientific assessment

Operational considerations related to the science objectives

Expedition 379 accomplished drilling and coring at two very successful sites on the continental rise of the Amundsen Sea. Drilling at Site U1532 on a large sediment drift (Resolution Drift) penetrated to 794 m (90% recovery), making this site the deepest drilled in West Antarctica with a ship-based rig and resulting in the largest overall recovered length of core and the highest percentage recovery in all of Antarctica. We collected almost continuous core from recent through the Pleistocene and Pliocene and into the upper Miocene. At Site U1533, we drilled to 383 m (70% recovery) into the more condensed sequence at the lower flank of the same sediment drift. The cores from both sites contain unique sample material suitable to study the cyclicity of ice sheet advance and retreat processes as well as bottom-water circulation and water mass changes. In particular, Site U1532 revealed a sequence of Pliocene lithofacies with an excellent paleomagnetic record for high-resolution climate change studies of the previously sparsely sampled Pacific margin of West Antarctica.

Despite the drilling success at both sites, the overall expedition experienced three difficulties that affected many of the scientific objectives of all five hypotheses of Proposal 839:

1. The extensive sea ice on the continental shelf prevented us from drilling any of the primary proposed sites located on the shelf. The two sites that we did successfully drill were added to the project in early 2018 after the record-setting austral summer sea ice cover in 2017/2018 extended over all approved primary and alternate sites from the proposal, forcing the creation of additional alternate plans. The sea ice remaining from 2018 became multiyear ice in 2019, limiting the breakout that could happen in a single season. During Expedition 379, sea ice was never at a level low enough for *JOIDES Resolution* to enter the shelf, even when sea ice became less concentrated between the continental rise and the open-water polynyas where many of the shelf sites are located.

2. On the continental rise, we faced a steady stream of icebergs of various sizes that approached the ship and frequently forced us to pause drilling or leave the hole entirely. The overall downtime caused by approaching icebergs was 50% of our time spent on site (Table **T1**). This large iceberg abundance in the Amundsen Sea during the austral summer was possibly unprecedented and may have been caused by major calving events of the ice shelves during the last 2–3 y.
3. Because of an injury to a member of the ship's crew, we had to cut the expedition short by 1 week. Before the unfortunate accident, which led to a medical evacuation, we intended to complete Site U1533 by coring through the mid-Miocene climate transition, complete downhole logging for the first time during the expedition, and collect APC cores at proposed Primary Site ASRE-05B near the foot of the continental slope, which had become accessible in the days before. Although all three of these goals likely would not have been possible in the last 7 days of the cruise, it is likely at least two of them would have been achieved.

Because of these three unexpected and extreme circumstances, we were unable to achieve many important objectives, including obtaining ice-proximal shelf records and collecting cores from the Mid-Miocene Climate Optimum, the Oligocene/Miocene boundary, and the Eocene–Oligocene transition. Drilling sites are needed to obtain ice-proximal records from these transitions for a full understanding of the proximal glacial history in this region, which is one of the key components of IODP's transect approach to understanding high-latitude climate history. The Expedition 379 sites were designed to obtain records of past warm deepwater incursions onto the shelf that are the cause of present melting. Models suggest that the current incursion of warm deepwater to the base of the ice is an unsustainable situation, but we do not yet have records showing whether warm water has encroached onto the shelf prior to the Holocene and, if so, how the WAIS responded. The study of such records from the shelf is one of the central scientific objectives of the proposal for Expedition 379.

Preliminary assessment of scientific objectives

The scientific objectives for this expedition were built on five hypotheses about the dynamics of the WAIS and related paleoenvironmental and paleoclimatic conditions. Based on a preliminary analysis of the core material and data collected during the expedition, we assess each of the five hypotheses below.

From the outset, Expedition 379 included a wide range of primary and alternate sites to allow for drilling in a range of sea ice conditions. All five objectives were addressed at most sites, both primary and alternate. However, the third tier of drill targets on the continental rise, proposed in case of extreme sea ice cover, could only be used to address the first three hypotheses in a more indirect way, and these third-tier sites were the only sites achieved during Expedition 379. Nonetheless, high-quality core recovery combined with slight modifications to our research approach allows each of the five hypotheses to be addressed to some degree.

Sites U1532 and U1533 are located on a sediment drift, the Resolution Drift, on the continental rise north of the Amundsen Sea Embayment shelf edge (Figure **F1**). Coring at both sites recovered relatively undisturbed sequences from the late Miocene to Quaternary.

Coring at Site U1532 recovered silty clay(stone) with dispersed sand and gravel and variable biogenic content in five holes to a core depth of 787 m (Figures **F4**, **F8**). Linear sedimentation rate calculated between magnetostratigraphic age control points shows a significant downcore increase in sedimentation rate that averages ~2 cm/ky in the Pleistocene, ~18 cm/ky in the middle Pliocene, and ~41 cm/ky during the latest Miocene to early Pliocene. The highest sedimentation rate (~61 cm/ky) is documented for the time between 4.49 and 4.63 Ma. The lowest sedimentation rate (~10 cm/ky) is calculated for the early Pliocene between 4.63 and 4.80 Ma and may indicate an episodic decrease in sediment flux to the site or possibly the presence of a short hiatus in this interval.

Sediments recovered at Site U1533 consist mainly of silty clay(stone) with varying biogenic content and amounts of bioturbation and rare occurrences of diamict and conglomerate intervals. Four holes were drilled at this site, reaching a total core depth of 382.6 m (Figures **F6**, **F9**). Similar trends in sedimentation rates are documented at Sites U1532 and U1533, but sedimentation rates are two to three times lower at Site U1533. Linear sedimentation rate shows an overall downcore increase that averages ~1.4 cm/ky in the Pleistocene, ~5.4 cm/ky between ~4.5 and 2.6 Ma in the Pliocene, and ~15.5 cm/ky between ~5.2 and 4.5 Ma in the earliest Pliocene. The highest sedimentation rate (~21–22 cm/ky) at Site U1533 is recorded for the early Pliocene between 4.493 and 4.631 Ma and be-

Table T1. Expedition 379 hole summary. — = no data. **Download table in CSV format.**

Hole	Proposed site	Latitude	Longitude	Water depth (m)	Cored interval (m)	Core recovery (m)	Core recovery (%)	Drilled interval without coring (m)	Total penetration (m)	Time in hole (h)	Time in hole (days)
U1532A	ASRE-08A	68°36.6833′S	107°31.5003′W	3961.5	100.6	103.04	102	—	100.6	35.8	1.5
U1532B		68°36.6837′S	107°31.4696′W	3961.4	87.2	91.92	105	93.1	180.3	55.8	2.3
U1532C		68°36.6952′S	107°31.4721′W	3961.4	214	179.6	84	178.3	392.3	103.5	4.3
U1532D		68°36.6953′S	107°31.5015′W	3961.5	19.2	17.42	91	362.7	381.9	53.3	2.2
U1532E		68°36.4292′S	107°32.4613′W	3977.4	—	—	—	101.6	101.6	12.5	0.5
U1532F		68°36.6833′S	107°31.5303′W	3961.4	—	—	—	321.4	321.4	48.3	2
U1532G		68°36.6954′S	107°31.5299′W	3961.4	421.7	366.41	87	372.3	794	260.3	10.8
			Site U1532 totals:		842.7	758.39	90	1429.4	2272.1	569.3	23.7
U1533A	ASRE-09A	68°44.0168′S	109°0.6014′W	4180.8	28.5	29.54	104	—	28.5	37.5	1.6
U1533B		68°44.0994′S	109°3.0010′W	4190.1	357.1	250.78	70	25.5	382.6	206.5	8.6
U1533C		68°44.0696′S	109°1.5103′W	4183.1	7.7	7.74	101	—	7.7	4.5	0.2
U1533D		68°44.0727′S	109°1.4901′W	4183.9	40	40.01	100	—	40	31.8	1.3
			Site U1533 totals:		433.3	328.07	76	25.5	458.8	280.3	11.7
			Expedition 379 totals:		1276	1086.46	85	1454.9	2730.9	849.5	35.4

Figure F8. Composite lithostratigraphic summary, Holes U1532A–U1532D and U1532G. Lithostratigraphic subunits are divided based on changes in facies assemblages. MS = magnetic susceptibility.

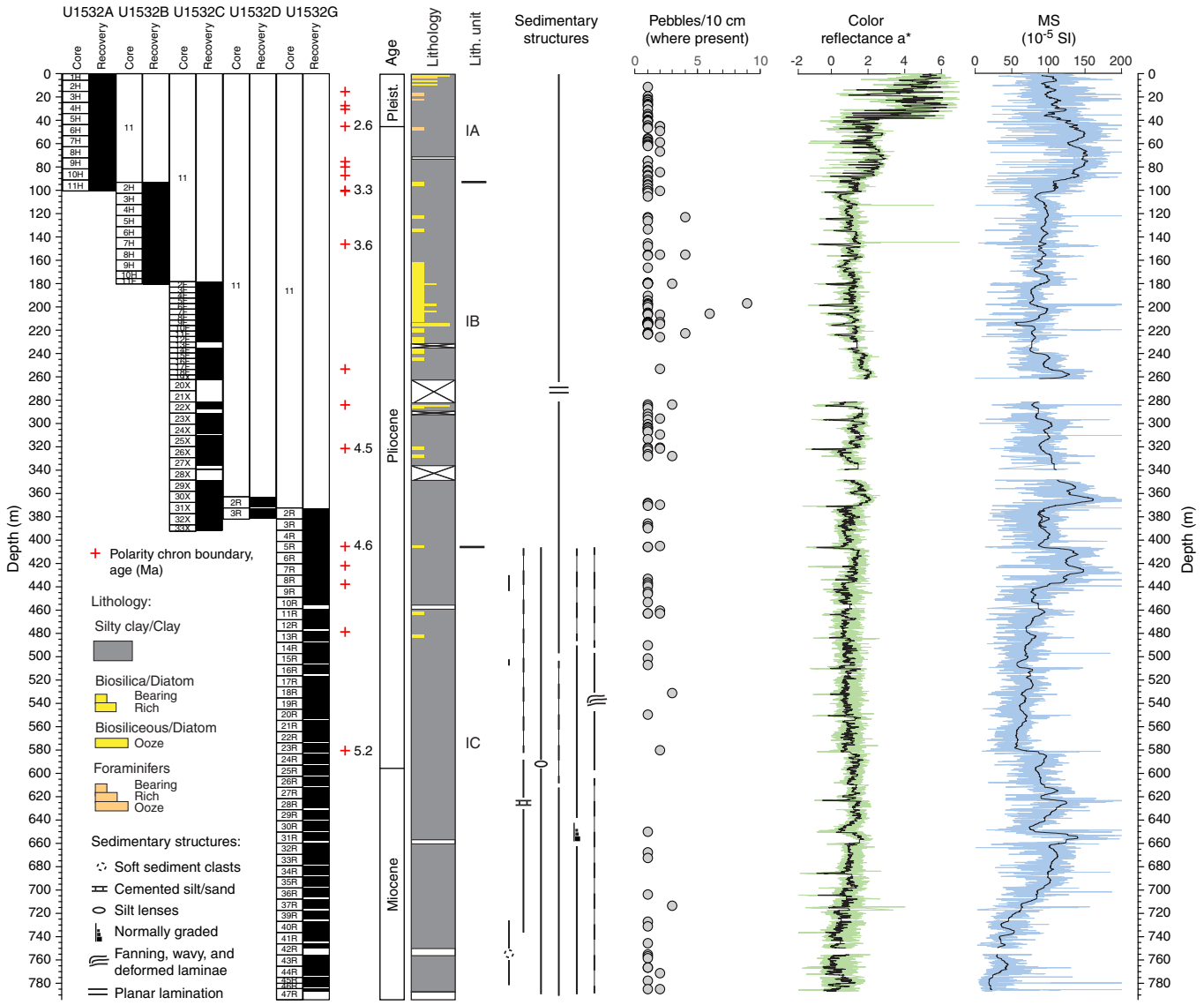

tween 4.997 and 5.235 Ma. The lowest sedimentation rate at Site U1533 (~3 cm/ky) is documented for a Pliocene phase between 4.631 and 4.799 Ma. A similar decrease in sedimentation rate is thus inferred for the same time interval at Sites U1532 and U1533, was also observed at Leg 178 Site 1095 on the western Antarctic Peninsula rise (Acton et al., 2002), and may indicate a regional decrease in terrigenous sediment flux between 4.63 and 4.80 Ma.

1. *Hypothesis H1: the WAIS responded to atmospheric and oceanic warming by a major retreat from the shelf or by even partial to full collapse.*

A primary goal of Expedition 379 is to reconstruct the glacial history of West Antarctica from the Paleogene to recent times with a focus on the dynamic behavior of the WAIS during the Neogene and Quaternary, especially possible partial or even full WAIS collapses. Particular emphasis is placed on studying the response of the WAIS at times when the pCO_2 in Earth's atmosphere exceeded 400 ppm and atmospheric and oceanic temperatures were higher than at present.

Recovery of core on the continental rise at Sites U1532 and U1533 cannot give a direct answer regarding the configuration of the WAIS on the shelf or retreat of its grounding line across the shelf. However, the sediments contained in the cores offer a range of initial clues about past ice sheet extent and retreat that will be elucidated in postcruise analyses. At both sites, coarse-grained sediments interpreted to be IRD were identified throughout all recovered time periods. Cyclicity is a dominant feature of the cores and is interpreted to represent alternations between warmer and colder periods, with sediments deposited during warmer periods being characterized by variable but generally higher microfossil abundance and higher IRD contents than sediments deposited during colder periods that are predominantly characterized by gray laminated terrigenous mud(stones). A revised age model will be completed after the expedition, and tuning of Expedition 379 data sets to precise time periods will follow. However, an initial comparison of these cycles with published upper Pleistocene records from the region (e.g., Hillenbrand et al., 2009) suggest that the units inter-

Figure F9. Composite lithostratigraphic summary, Holes U1533A–U1533D. Lithostratigraphic subunits are divided based on changes in facies assemblages.

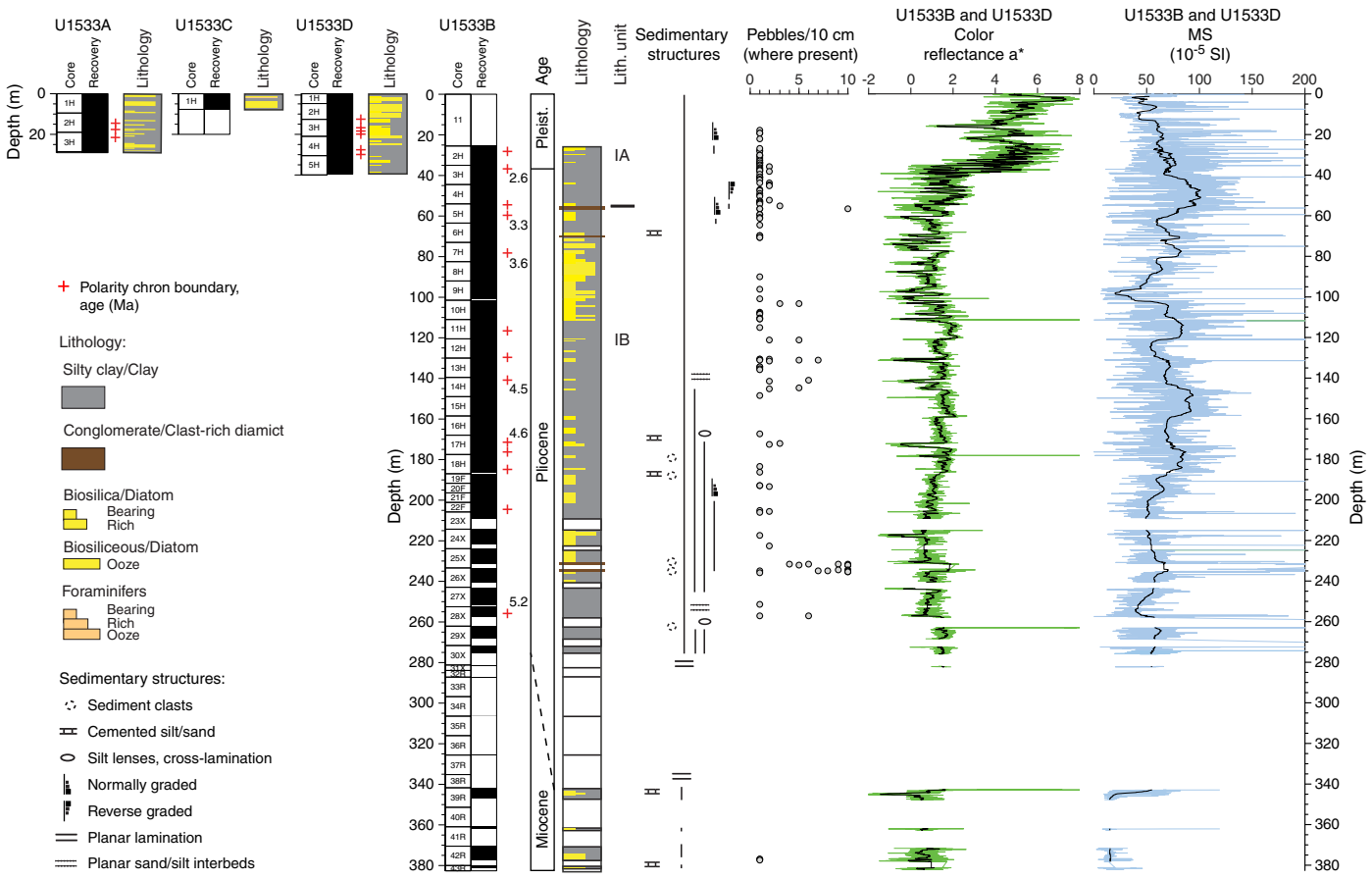

preted as records of warmer time intervals in the cores are tied to global interglacial periods and the units interpreted as deposits of colder periods are tied to global glacial periods. Postcruise work to determine IRD accumulation rates over time will allow identification of pulses of glacial sediment input that may be representative of major calving events.

More specific evidence of major reductions in the size of the WAIS or even its collapse will arise from studying the provenance of coarse-grained IRD and fine-grained detritus at the drill sites. IRD pulses often represent major calving events, although the signal can be ambiguous because it may simply be a local increase in accumulation or, barring detailed age constraints, a signal of decreased flux of fine-grained material. Therefore, layers rich in IRD will be targets for more detailed studies aimed at identifying the provenance of the IRD. Coarse grains will be identified by visual description and geochemical and mineralogical analyses that will also be applied to fine-grained detritus, including Sr-Nd signatures, to determine the source of glaciogenic sediment deposited on the Resolution Drift and thus to infer the extent of subglacial erosion and grounded ice in the West Antarctic hinterland. A change in provenance over time at the site will be an indication of varying positions of the grounding line. Specific isotopic signatures, including Pb isotopes, will be used to identify patterns of bedrock weathering that may indicate specific source rocks were exposed subaerially. Additionally, different clay mineral signatures with geochemical analyses (including Sr-Nd) in the fine-grained fraction may be identified as having come from specific regions onshore, allowing further identification of the source of sediment shed to the region and thus indicating how far the ice may have retreated.

These combined signals will allow reconstruction of the ice sheet since the late Miocene based on the amount and source of sediment shed to the drill sites. Results from ANDRILL Core AND-1B suggest repeated WAIS collapses during warm early middle Pliocene and Pleistocene interglacials (e.g., during MIS 31) (Naish et al., 2009; Pollard and DeConto, 2009; McKay et al., 2012; Villa et al., 2012). The hypothesis of WAIS collapse needs confirmation with a less ambiguous record from an outlet that is exclusively affected by ice draining the WAIS. The cores recovered during Expedition 379 may not give unambiguous information on past WAIS configuration because they were collected from a drift that has also been affected by lateral, bottom-current controlled sediment transport; however, the records of glaciogenic sediment delivery to the sites will give an integrated signal that will record major changes in ice sheet extent.

2. *Hypothesis H2: ice-proximal records of ice sheet dynamics in the Amundsen Sea correlate with global records of ice-volume changes and proxy records for atmospheric and ocean temperatures.*

A goal of Expedition 379 is to correlate the WAIS-proximal records of ice sheet dynamics in the Amundsen Sea with global records of ice-volume changes and proxy records for air and seawater temperatures. As described above, the initial interpretation of cores from Sites U1532 and U1533 shows repeated alternations between

different facies interpreted to represent glacial–interglacial cycles. Comparison with dated gravity and piston cores nearby (e.g., Hillenbrand et al., 2002, 2009) suggest that the cycles identified in cores from both sites are correlative with global oxygen-isotope records. The pattern holds at least as far back as MIS 35, and thus several "superinterglacials" have been recovered. Ongoing work will focus on tuning the age model, particularly for Pliocene warm intervals that are not yet well constrained, to confirm these initial interpretations and allow more detailed analyses, including deconvolving the glacial–interglacial signals from what may be independent changes in ocean currents delivering sediment to the drill sites.

Work on proxies will be conducted to determine paleoceanographic characteristics, including surface water temperature, salinity, current speed, and water mass origins. These data, which are independent of the specific age models, will allow the record of ice sheet fluctuations to be tied to local temperature and current information as well as to the global records of ice volume.

3. *Hypothesis H3: the stability of marine-based WAIS margins is and has been controlled by warm deepwater incursions onto the shelf.*

Today, the dramatic Amundsen Sea sector ice loss is attributed to incursions of warm CDW reaching the base of the ice shelves fringing the WAIS (Joughin et al., 2014). Such incursions have been identified in the Holocene (Hillenbrand et al., 2017; Minzoni et al., 2017) and recent sediments (Smith et al., 2017), but it is unclear how often such incursions have happened further in the past or how the ice may have responded. Therefore, another goal of Expedition 379 is to study the relationship between incursions of CDW onto the continental shelf of the Amundsen Sea Embayment and the stability of marine-based ice sheet margins under such warm-water conditions. Postcruise work will try to fingerprint water masses flowing across the drill site, and multiple proxies will estimate surface water temperature, including lipid paleothermometers, trace metal data from calcareous foraminifer shells, and diatom-based temperature proxies. However, most of these analyses will yield details of either surface water or bottom-water mass properties that may not directly be linked to changes in CDW upwelling onto the Amundsen Sea shelf. The difference in Pleistocene diatom accumulation between Sites U1532 and U1533 cannot be explained by local surface water productivity differences. Consequently, the differences may result from enhanced advection of pelagic diatoms at Site U1533. This process will be explored as a potential signal of CDW changes over time. Estimates of broad-scale temperature proxy changes over time will be compared with the IRD signal and other records of ice sheet change, allowing correlation between temperature at the drill sites and ice sheet behavior.

4. *Hypothesis H4: major WAIS advances onto the middle and outer shelf have occurred since the middle Miocene.*

One of the aims during Expedition 379 was to obtain records from various sites on the Amundsen Sea Embayment shelf from unconformities within strata that document frequent advance and retreat of grounded ice from the late Miocene until the Pliocene/Pleistocene. Seismic data reveal progradational and aggradational deposition on the outer shelf and slope probably since the mid-Miocene (e.g., Nitsche et al., 1997, 2000; Hochmuth and Gohl, 2013; Gohl et al., 2013b). The seismic stratigraphic age model of the shelf sequences by Gohl et al. (2013b) is only constrained by far-distance correlation of seismic reflection characteristics and patterns with those observed and age-dated from the Ross Sea shelf (e.g., De Santis et al., 1999) due to the lack of deep drill sites on the Amundsen Sea shelf. We were unable to access the open-water polynyas on the shelf with *JOIDES Resolution* during Expedition 379 because of sea ice on the outer shelf, which prevented us from obtaining such direct shelf records.

The drill cores from both rise sites, however, recovered sediments of terrigenous origin intercalated or mixed with pelagic and hemipelagic deposits. In particular, Site U1533, which is located near a deep-sea channel running from the lower continental slope to the abyssal plain, contains graded beds as well as clasts transported downslope from the shelf by turbidity currents or other gravitational transport processes.

The association of lithologic facies in both sites predominantly reflects the interplay of downslope and contouritic sediment supply with more pelagic sediment input during phases of seasonal open-marine conditions, which are inferred from a greater amount of biogenic material documenting relatively sustained periods of relatively high marine productivity. Recovered dispersed granules and pebbles, clasts, and discontinuous bands of coarse sand and granules in the cores are interpreted to indicate persistent but likely low-intensity ice rafting that may have increased periodically during warmer periods. Because these observations can be made throughout the Pleistocene and Pliocene and into the upper Miocene, we can infer from drilling that grounded ice frequently covered most of the Amundsen Sea shelf since at least the late Miocene.

Despite the lack of drill cores from the shelf, our records from the continental rise reveal the timing of glacial advances onto the shelf and thus the existence of a continent-wide ice sheet in West Antarctica for prolonged periods since at least the late Miocene. Hypotheses of earlier phases of WAIS expansion in the Amundsen Sea sector remain untested by drill records.

5. *Hypothesis H5: the first WAIS advance onto the inner Amundsen Sea continental shelf occurred during the Oligocene and was related to the uplift of Marie Byrd Land.*

The relationship between the onset of major West Antarctic glaciation and the continental paleotopography necessary for growing a substantial ice sheet has so far only been addressed by numerical modeling (DeConto and Pollard, 2003; Wilson et al., 2013). Such modeling indicates that an elevated Marie Byrd Land dome might be required for a large ice sheet to form in the Amundsen Sea/Marie Byrd Land sector. Seismological models show that a low-velocity, presumably hotter than normal mantle exists beneath Marie Byrd Land today (e.g., Lloyd et al., 2015). An objective of Expedition 379 was to reveal evidence from drill records that will allow reconstruction of the timing and rates of an uplift that has been inferred by studies of the Marie Byrd Land dome exhumation and erosion history (e.g., Rocchi et al., 2006; Wilson and Luyendyk, 2009; Wilson et al., 2012, 2013; Spiegel et al., 2016). The latest thermochronological study suggests an uplift not earlier than the early Miocene (Spiegel et al., 2016).

Although we were unable to drill cores for detailed provenance and thermochronological analyses of samples from the shelf, cores from both rise sites contain abundant coarse-fraction sediments and clasts of plutonic origin transported by either downslope processes or ice rafting. The common lithic types are polycrystalline quartz and K-feldspar granite. Biotite-bearing leucogranite and diorite are also present. If detailed provenance studies confirm our preliminary assessment that the origin of these samples is plutonic

bedrock from Marie Byrd Land, their thermochronological record will potentially reveal timing and rates of denudation and erosion linked to crustal uplift.

The chronostratigraphy of both drill sites enables the generation of a seismic sequence stratigraphy not only for the Amundsen Sea rise but also for the area offshore the Amundsen Sea Embayment and farther west along the Marie Byrd Land margin into the easternmost Ross Sea through a connecting network of seismic lines. A detailed analysis of correlated seismic unit boundaries and unconformities will allow reconstruction of the Marie Byrd Land dome uplift at least back to the earliest age-dated horizons of the late Miocene and, with an appropriate seismic stratigraphic age model using estimates on earlier sedimentation rates, possibly even back to the Oligocene or earlier.

In addressing the objectives of this hypothesis, the thermochronological analyses and seismic sequence stratigraphy will make use of the drilled core samples and the core data from independent methods to test the hypothesis of the Marie Byrd Land uplift and its role in early ice sheet evolution.

References

Acton, G.D., Guyodo, Y., and Brachfeld, S.A., 2002. Magnetostratigraphy of sediment drifts on the continental rise of West Antarctica (ODP Leg 178, Sites 1095, 1096, and 1101). *In* Barker, P.F., Camerlenghi, A., Acton, G.D., and Ramsay, A.T.S. (Eds.), *Proceedings of the Ocean Drilling Program, Scientific Results,* 178: College Station, TX (Ocean Drilling Program), 1–61. **https://doi.org/10.2973/odp.proc.sr.178.235.2002**

Alonso, B., Anderson, J.B., Diaz, J.I., and Bartek, L.R., 1992. Pliocene–Pleistocene seismic stratigraphy of the Ross Sea: evidence for multiple ice sheet grounding episodes. *In* Elliot, D.H. (Ed.), *Antarctic Research Series* (Volume 57): *Contributions to Antarctic Research III:* Washington DC (American Geophysical Union), 93–103. **https://agupubs.onlinelibrary.wiley.com/doi/10.1029/AR057p0093**

Anderson, J.B., and Bartek, L.R., 1992. Cenozoic glacial history of the Ross Sea revealed by intermediate resolution seismic reflection data combined with drill site information. *In* Kennett J.P., and Warnke D. (Eds.), *Antarctic Research Series* (Volume 56): *The Antarctic Paleoenvironment: A Perspective on Global Change: Part One:* Washington DC (American Geophysical Union), 231–263. **https://agupubs.onlinelibrary.wiley.com/doi/pdf/10.1029/AR056p0231**

Anderson, J.B., Warny, S., Askin, R.A., Wellner, J.S., Bohaty, S.M., Kirshner, A.E., Livsey, D.N., et al., 2011. Progressive Cenozoic cooling and the demise of Antarctica's last refugium. *Proceedings of the National Academy of Sciences of the United States of America,* 108(28):11356–11360. **https://doi.org/10.1073/pnas.1014885108**

Anderson, J.B., and Wellner, J.S. (Eds.), 2011. *Tectonic, Climatic, and Cryospheric Evolution of the Antarctic Peninsula:* Washington, DC (American Geophysical Union). **https://doi.org/10.1029/SP063**

Arneborg, L., Wåhlin, A.K., Björk, G., Liljebladh, B., and Orsi, A.H., 2012. Persistent inflow of warm water onto the central Amundsen shelf. *Nature Geoscience,* 5(12):876–880. **https://doi.org/10.1038/ngeo1644**

Arrigo, K.R., van Dijken, G.L., and Bushinsky, S., 2008. Primary production in the Southern Ocean, 1997–2006. *Journal of Geophysical Research: Oceans,* 113(C8):C08004. **https://doi.org/10.1029/2007JC004551**

Arrigo, K.R., van Dijken, G.L., and Strong, A.L., 2015. Environmental controls of marine productivity hot spots around Antarctica. *Journal of Geophysical Research: Oceans,* 120(8):5545–5565. **https://doi.org/10.1002/2015JC010888**

Barker, P.F., and Camerlenghi, A., 2002. Glacial history of the Antarctic Peninsula from Pacific margin sediments. *In* Barker, P.F., Camerlenghi, A., Acton, G.D., and Ramsay, A.T.S. (Eds.), *Proceedings of the Ocean Drilling Program, Scientific Results,* 178: College Station, TX (Ocean Drilling Program), 1–40. **https://doi.org/10.2973/odp.proc.sr.178.238.2002**

Bart, P.J., 2001. Did the Antarctic ice sheets expand during the early Pliocene? *Geology,* 29(1):67–70. **https://doi.org/10.1130/0091-7613(2001)029<0067:DTAISE>2.0.CO;2**

Bart, P.J., and Anderson, J.B., 2000. Relative temporal stability of the Antarctic ice sheets during the late Neogene based on the minimum frequency of outer shelf grounding events. *Earth and Planetary Science Letters,* 182(3–4):259–272. **https://doi.org/10.1016/S0012-821X(00)00257-0**

Bart, P.J., Egan, D., and Warny, S.A., 2005. Direct constraints on Antarctic Peninsula Ice Sheet grounding events between 5.12 and 7.94 Ma. *Journal of Geophysical Research: Earth Surface,* 110(F4):F04008. **https://doi.org/10.1029/2004JF000254**

Bart, P.J., and Iwai, M., 2012. The overdeepening hyphothesis: how erosional modification of the marine-scape during the early Pliocene altered glacial dynamics on the Antarctic Peninsula's Pacific margin. *Palaeogeography, Palaeoclimatology, Palaeoecology,* 335–336:42–51. **https://doi.org/10.1016/j.palaeo.2011.06.010**

Bartek, L.R., Vail, P.R., Anderson, J.B., Emmet, P.A., and Wu, S., 1991. Effect of Cenozoic ice sheet fluctuations in Antarctica on the stratigraphic signature of the Neogene. *Journal of Geophysical Research: Solid Earth,* 96(B4):6753–6778. **https://doi.org/10.1029/90JB02528**

Carter, A., Riley, T.R., Hillenbrand, C.-D., and Rittner, M., 2017. Widespread Antarctic glaciation during the late Eocene. *Earth and Planetary Science Letters,* 458:49–57. **https://doi.org/10.1016/j.epsl.2016.10.045**

Chow, J.M., and Bart, P.J., 2003. West Antarctic Ice Sheet grounding events on the Ross Sea outer continental shelf during the middle Miocene. *Palaeogeography, Palaeoclimatology, Palaeoecology,* 198(1–2):169–186. **https://doi.org/10.1016/S0031-0182(03)00400-0**

Cook, C.P., van de Flierdt, T., Williams, T., Hemming, S.R., Iwai, M., Kobayashi, M., Jimenez-Espejo, F.J., et al., 2013. Dynamic behaviour of the East Antarctic Ice Sheet during Pliocene warmth. *Nature Geoscience,* 6(9):765–769. **https://doi.org/10.1038/ngeo1889**

Cowan, E.A., Hillenbrand, C.-D., Hassler, L.E., and Ake, M.T., 2008. Coarse-grained terrigenous sediment deposition on continental rise drifts: a record of Plio–Pleistocene glaciation on the Antarctica Peninsula. *Palaeogeography, Palaeoclimatology, Palaeoecology,* 265(3–4):275–291. **https://doi.org/10.1016/j.palaeo.2008.03.010**

De Santis, L., Anderson, J.B., Brancolini, G., and Zayatz, I., 1997. Glaciomarine deposits on the continental shelf of Ross Sea, Antarctica. *In* Davies, T.A., Bell, T., Cooper, A.K., Josenhans, H., Polyak, L., Solheim, A., Stoker, M.S., and Stravers, J.A. (Eds.), *Glaciated Continental Margins: An Atlas of Acoustic Images*: London (Chapman & Hall), 110–113. **https://doi.org/10.1007/978-94-011-5820-6_41**

De Santis, L., Prato, S., Brancolini, G., Lovo, M., and Torelli, L., 1999. The eastern Ross Sea continental shelf during the Cenozoic: implications for the West Antarctic ice sheet development. *Global and Planetary Change,* 23(1–4):173–196. **https://doi.org/10.1016/S0921-8181(99)00056-9**

DeConto, R.M., and Pollard, D., 2003. Rapid Cenozoic glaciation of Antarctica induced by declining atmospheric CO_2. *Nature,* 421(6920):245–249. **https://doi.org/10.1038/nature01290**

DeConto, R.M., and Pollard, D., 2016. Contribution of Antarctica to past and future sea-level rise. *Nature,* 531(7596):591–597. **https://doi.org/10.1038/nature17145**

Dowdeswell, J.A., Evans, J., Ó Cofaigh, C., and Anderson, J.B., 2006. Morphology and sedimentary processes on the continental slope off Pine Island Bay, Amundsen Sea, West Antarctica. *Geological Society of America Bulletin,* 118(5–6):606–619. **https://doi.org/10.1130/B25791.1**

Dutrieux, P., De Rydt, J., Jenkins, A., Holland, P.R., Ha, H.K., Lee, S.H., Steig, E.J., Ding, Q., Abrahamsen, E.P., and Schröder, M., 2014. Strong sensitivity of Pine Island ice-shelf melting to climatic variability. *Science,* 343(6167):174–178. **https://doi.org/10.1126/science.1244341**

Ehrmann, W., Hillenbrand, C.-D., Smith, J.A., Graham, A.G.C., Kuhn, G., and Larter, R.D., 2011. Provenance changes between recent and glacial-time sediments in the Amundsen Sea Embayment, West Antarctica: clay mineral assemblage evidence. *Antarctic Science,* 23(5):471–486. **https://doi.org/10.1017/S0954102011000320**

Escutia, C., Bárcena, M.A., Lucchi, R.G., Romero, O., Ballegeer, A.M., Gonzalez, J.J., and Harwood, D.M., 2009. Circum-Antarctic warming events

between 4 and 3.5 Ma recorded in marine sediments from the Prydz Bay (ODP Leg 188) and the Antarctic Peninsula (ODP Leg 178) margins. *Global and Planetary Change,* 69(3):170–184. **https://doi.org/10.1016/j.gloplacha.2009.09.003**

Eyles, N., Daniels, J., Osterman, L.E., and Januszczak, N., 2001. Ocean Drilling Program Leg 178 (Antarctic Peninsula): sedimentology of glacially influenced continental margin topsets and foresets. *Marine Geology,* 178(1–4):135–156. **https://doi.org/10.1016/S0025-3227(01)00184-0**

Fretwell, P., Pritchard, H.D., Vaughan, D.G., Bamber, J.L., Barrand, N.E., Bell, R., Bianchi, C., et al., 2013. Bedmap2: improved ice bed, surface and thickness datasets for Antarctica. *The Cryosphere,* 7(1):375–393. **https://doi.org/10.5194/tc-7-375-2013**

Gohl, K., Denk, A., Eagles, G., and Wobbe, F., 2013a. Deciphering tectonic phases of the Amundsen Sea Embayment shelf, West Antarctica, from a magnetic anomaly grid. *Tectonophysics,* 585:113–123. **https://doi.org/10.1016/j.tecto.2012.06.036**

Gohl, K., Freudenthal, T., Hillenbrand, C.-D., Klages, J., Larter, R., Bickert, T., Bohaty, S., et al., 2017. MeBo70 seabed drilling on a polar continental shelf: operational report and lessons from drilling in the Amundsen Sea Embayment of West Antarctica. *Geochemistry, Geophysics, Geosystems,* 18(11):4235–4250. **https://doi.org/10.1002/2017GC007081**

Gohl, K., Uenzelmann-Neben, G., Larter, R.D., Hillenbrand, C.-D., Hochmuth, K., Kalberg, T., Weigelt, E., Davy, B., Kuhn, G., and Nitsche, F.O., 2013b. Seismic stratigraphic record of the Amundsen Sea Embayment shelf from pre-glacial to recent times: evidence for a dynamic West Antarctic Ice Sheet. *Marine Geology,* 344:115–131. **https://doi.org/10.1016/j.margeo.2013.06.011**

Gradstein, F.M., Ogg, J.G., Schmitz, M.D., and Ogg, G.M. (Eds.), 2012. *The Geological Time Scale 2012:* Amsterdam (Elsevier). **https://doi.org/10.1016/C2011-1-08249-8**

Graham, A.G.C., Larter, R.D., Gohl, K., Dowdeswell, J.A., Hillenbrand, C.-D., Smith, J.A., Evans, J., Kuhn, G., and Deen, T., 2010. Flow and retreat of the Late Quaternary Pine Island-Thwaites palaeo-ice stream, West Antarctica. *Journal of Geophysical Research: Earth Surface,* 115(F3):F03025. **https://doi.org/10.1029/2009JF001482**

Graham, A.G.C., Larter, R.D., Gohl, K., Hillenbrand, C.-D., Smith, J.A., and Kuhn, G., 2009. Bedform signature of a West Antarctic palaeo-ice stream reveals a multi-temporal record of flow and substrate control. *Quaternary Science Reviews,* 28(25–26):2774–2793. **https://doi.org/10.1016/j.quascirev.2009.07.003**

Haywood, A.M., Chandler, M.A., Valdes, P.J., Salzmann, U., Lunt, D.J., and Dowsett, H.J., 2009. Comparison of mid-Pliocene climate predictions produced by the HadAM3 and GCMAM3 general circulation models. *Global and Planetary Change,* 66(3–4):208–224. **https://doi.org/10.1016/j.gloplacha.2008.12.014**

Hepp, D.A., Mörz, T., and Grützner, J., 2006. Pliocene glacial cyclicity in a deep-sea sediment drift (Antarctic Peninsula Pacific Margin). *Palaeogeography, Palaeoclimatology, Palaeoecology,* 231(1–2):181–198. **https://doi.org/10.1016/j.palaeo.2005.07.030**

Hepp, D.A., Mörz, T., Hensen, C., Frederichs, T., Kasten, S., Riedinger, N., and Hay, W.W., 2009. A late Miocene–early Pliocene Antarctic deepwater record of repeated iron reduction events. *Marine Geology,* 266(1–4):198–211. **https://doi.org/10.1016/j.margeo.2009.08.006**

Hillenbrand, C.-D., and Cortese, G., 2006. Polar stratification: a critical view from the Southern Ocean. *Palaeogeography, Palaeoclimatology, Palaeoecology,* 242(3–4):240–252. **https://doi.org/10.1016/j.palaeo.2006.06.001**

Hillenbrand, C.-D., and Ehrmann, W., 2005. Late Neogene to Quaternary environmental changes in the Antarctic Peninsula region: evidence from drift sediments. *Global and Planetary Change,* 45(1–3):165–191. **https://doi.org/10.1016/j.gloplacha.2004.09.006**

Hillenbrand, C.-D., Fütterer, D.K., Grobe, H., and Frederichs, T., 2002. No evidence for a Pleistocene collapse of the West Antarctic Ice Sheet from continental margin sediments recovered in the Amundsen Sea. *Geo-Marine Letters,* 22(2):51–59. **https://doi.org/10.1007/s00367-002-0097-7**

Hillenbrand, C.-D., Kuhn, G., and Frederichs, T., 2009. Record of a mid-Pleistocene depositional anomaly in West Antarctic continental margin sediments: an indicator for ice-sheet collapse? *Quaternary Science Reviews,* 28(13–14):1147–1159. **https://doi.org/10.1016/j.quascirev.2008.12.010**

Hillenbrand, C.-D., Kuhn, G., Smith, J.A., Gohl, K., Graham, A.G.C., Larter, R.D., Klages, J.P., et al., 2013. Grounding-line retreat of the West Antarctic Ice Sheet from inner Pine Island Bay. *Geology,* 41(1):35–38. **https://doi.org/10.1130/G33469.1**

Hillenbrand, C.-D., Moreton, S.G., Caburlotto, A., Pudsey, C.J., Lucchi, R.G., Smellie, J.L., Benetti, S., Grobe, H., Hunt, J.B., and Larter, R.D., 2008. Volcanic time-markers for Marine Isotopic Stages 6 and 5 in Southern Ocean sediments and Antarctic ice cores: implications for tephra correlations between palaeoclimatic records. *Quaternary Science Reviews,* 27(5–6):518–540. **https://doi.org/10.1016/j.quascirev.2007.11.009**

Hillenbrand, C.-D., Smith, J.A., Hodell, D.A., Greaves, M., Poole, C.R., Kender, S., Williams, M., et al., 2017. West Antarctic Ice Sheet retreat driven by Holocene warm water incursions. *Nature,* 547(7661):43–48. **https://doi.org/10.1038/nature22995**

Hochmuth, K., and Gohl, K., 2013. Glaciomarine sedimentation dynamics of the Abbot glacial trough of the Amundsen Sea Embayment shelf, West Antarctica. *In* Hambrey, M.J., Barker, P.F., Barrett, P.J., Bowman, V., Davies, B., Smellie, J.L., and Tranter, M. (Eds.), *Antarctic Palaeoenvironments and Earth-Surface Processes.* Geological Society Special Publication, 381:233–244. **https://doi.org/10.1144/SP381.21**

Holden, P.B., Edwards, N.R., Wolff, E.W., Lang, N.J., Singarayer, J.S., Valdes, P.J., and Stocker, T.F., 2010. Interhemispheric coupling, the West Antarctic Ice Sheet and warm Antarctic interglacials. *Climate of the Past,* 6(4):431–443. **https://doi.org/10.5194/cp-6-431-2010**

Hollister, C.D., and Craddock, C., 1976. Introduction, principal results—Leg 35, Deep Sea Drilling Project. *In* Hollister, C.D., Craddock, C., et al., *Initial Reports of the Deep Sea Drilling Project,* 35: Washington, DC (U.S. Government Printing Office), 5–14. **https://doi.org/10.2973/dsdp.proc.35.101.1976**

Hughes, T.J., 1981. The weak underbelly of the West Antarctic Ice Sheet. *Journal of Glaciology*, 27(97):518–525. **https://doi.org/10.3189/S002214300001159X**

Intergovernmental Panel on Climate Change, 2007. *Climate Change 2007: Synthesis Report. Contribution of Working Groups I, II and III to the Fourth Assessment Report of the Intergovernmental Panel on Climate Change*: Geneva (Intergovernmental Panel on Climate Change). **http://climate.calcommons.org/bib/climate-change-2007-synthesis-report-contribution-working-groups-i-ii-and-iii-fourth-assessment**

Intergovernmental Panel on Climate Change, 2013. Summary for policymakers. *In* Stocker, T.F., Qin, D., Plattner, G.-K., Tignor, M., Allen, S.K., Boschung, J., Nauels, A., Xia, Y., Bex, V., and Midgley, P.M. (Eds.), *Climate Change 2013: The Physical Science Basis. Contribution of Working Group I to the Fifth Assessment Report of the Intergovernmental Panel on Climate Change:* Cambridge, United Kingdom (Cambridge University Press), 3–29. **http://www.climatechange2013.org/images/report/WG1AR5_SPM_FINAL.pdf**

Intergovernmental Panel on Climate Change, 2018. Summary for policymakers. *In* Masson-Delmotte, V., Zhai, P., Pörtner, H.-O., Roberts, D., Skea, J., Shukla, P.R., Pirani, A., et al. (Eds.), *Global Warming of 1.5°C:* Geneva (Intergovernmental Panel on Climate Change). **https://www.ipcc.ch/site/assets/uploads/sites/2/2018/07/SR15_SPM_version_stand_alone_LR.pdf**

Jacobs, S., Giulivi, C., Dutrieux, P., Rignot, E., Nitsche, F., and Mouginot, J., 2013. Getz Ice Shelf melting response to changes in ocean forcing. *Journal of Geophysical Research: Oceans,* 118(9):4152–4168. **https://doi.org/10.1002/jgrc.20298**

Jacobs, S., Jenkins, A., Hellmer, H., Giulivi, C., Nitsche, F., Huber, B., and Guerrero, R., 2012. The Amundsen Sea and the Antarctic Ice Sheet. *Oceanography*, 25(3):154–163. **https://doi.org/10.5670/oceanog.2012.90**

Jacobs, S.S., Jenkins, A., Giulivi, C.F., and Dutrieux, P., 2011. Stronger ocean circulation and increased melting under Pine Island Glacier ice shelf. *Nature Geoscience,* 4(8):519–523. **https://doi.org/10.1038/ngeo1188**

Jakobsson, M., Anderson, J.B., Nitsche, F.O., Dowdeswell, J.A., Gyllencreutz, R., Kirchner, N., Mohammad, R., et al., 2011. Geological record of ice shelf break-up and grounding line retreat, Pine Island Bay, West Antarctica. *Geology,* 39(7):691–694. **https://doi.org/10.1130/G32153.1**

Jakobsson, M., Anderson, J.B., Nitsche, F.O., Gyllencreutz, R., Kirshner, A.E., Kirchner, N., O'Regan, M., Mohammad, R., and Eriksson, B., 2012. Ice sheet retreat dynamics inferred from glacial morphology of the central Pine Island Bay Trough, West Antarctica. *Quaternary Science Reviews,* 38:1–10. **https://doi.org/10.1016/j.quascirev.2011.12.017**

Jenkins, A., Dutrieux, P., Jacobs, S., Steig, E.J., Gudmundsson, G.H, Smith, J., and Heywood, K.J., 2016. Decadal ocean forcing and Antarctic Ice Sheet response: lessons from the Amundsen Sea. *Oceanography,* 29(4):58–69. **https://doi.org/10.5670/oceanog.2016.103**

Joughin, I., and Alley, R.B., 2011. Stability of the West Antarctic Ice Sheet in a warming world. *Nature Geoscience,* 4(8):506–513. **https://doi.org/10.1038/ngeo1194**

Joughin, I., Alley, R.B., and Holland, D.M., 2012. Ice-sheet response to oceanic forcing. *Science,* 338(6111):1172–1176. **https://doi.org/10.1126/science.1226481**

Joughin, I., Smith, B.E., and Medley, B., 2014. Marine ice sheet collapse potentially under way for the Thwaites Glacier Basin, West Antarctica. *Science,* 344(6185):735–738. **https://doi.org/10.1126/science.1249055**

Kim, T.W., Ha, H.K., Wåhlin, A.K., Lee, S.H., Kim, C.S., Lee, J.H., and Cho, Y.K., 2017. Is Ekman pumping responsible for the seasonal variation of warm circumpolar deep water in the Amundsen Sea? *Continental Shelf Research,* 132:38–48. **https://doi.org/10.1016/j.csr.2016.09.005**

Kirshner, A.E., Anderson, J.B., Jakobsson, M., O'Regan, M., Majewski, W., and Nitsche, F.O., 2012. Post-LGM deglaciation in Pine Island Bay, West Antarctica. *Quaternary Science Reviews,* 38:11–26. **https://doi.org/10.1016/j.quascirev.2012.01.017**

Klages, J.P., Kuhn, G., Hillenbrand, C.-D., Smith, J.A., Graham, A.G.C., Nitsche, F.O., Frederichs, T., Jernas, P.E., Gohl, K., and Wacker, L., 2017. Limited grounding-line advance onto the West Antarctic continental shelf in the easternmost Amundsen Sea Embayment during the last glacial period. *PLoS One,* 12(7):e0181593. **https://doi.org/10.1371/journal.pone.0181593**

Konfirst, M.A., Scherer, R.P., Hillenbrand, C.-D., and Kuhn, G., 2012. A marine diatom record from the Amundsen Sea—insights into oceanographic and climatic response to the Mid-Pleistocene Transition in the West Antarctic sector of the Southern Ocean. *Marine Micropaleontology,* 92–93:40–51. **https://doi.org/10.1016/j.marmicro.2012.05.001**

Larter, R.D., Anderson, J.B., Graham, A.G.C., Gohl, K., Hillenbrand, C.-D., Jakobsson, M., Johnson, J.S., et al., 2014. Reconstruction of changes in the Amundsen Sea and Bellingshausen Sea sector of the West Antarctic Ice Sheet since the Last Glacial Maximum. *Quaternary Science Reviews,* 100:55–86. **https://doi.org/10.1016/j.quascirev.2013.10.016**

Larter, R.D., Graham, A.G.C., Gohl, K., Kuhn, G., Hillenbrand, C.-D., Smith, J.A., Deen, T.J., Livermore, R.A., and Schenke, H.-W., 2009. Subglacial bedforms reveal complex basal regime in a zone of paleo-ice stream convergence, Amundsen Sea Embayment, West Antarctica. *Geology,* 37(5):411–414. **https://doi.org/10.1130/G25505A.1**

Larter, R.D., Rebesco, M., Vanneste, L.E., Gamboa, L.A.P., and Barker, P., 1997. Cenozoic tectonic, sedimentary and glacial history of the continental shelf west of Graham Land, Antarctic Peninsula. *In* Cooper, A.K., Barker, P.F., and Brancolini, G. (Eds.), *Geology and Seismic Stratigraphy of the Antarctic Margin* (Part 2). Antarctic Research Series, 71:1–27. **https://doi.org/10.1029/AR071p0001**

Le Masurier, W.E., and Rex, D.C., 1991. The Marie Byrd Land volcanic province and its relation to the Cainozoic West Antarctic rift system. *In* Tingey, R.J. (Ed.), *The Geology of Antarctica*. Oxford Monographs on Geology and Geophysics, 17:249–284.

Lindeque, A., Gohl, K., Henrys, S., Wobbe, F., and Davy, B., 2016a. Seismic stratigraphy along the Amundsen Sea to Ross Sea continental rise: a cross-regional record of pre-glacial to glacial processes of the West Antarctic margin. *Palaeogeography, Palaeoclimatology, Palaeoecology,* 443:183–202. **https://doi.org/10.1016/j.palaeo.2015.11.017**

Lindeque, A., Gohl, K., Wobbe, F., and Uenzelmann-Neben, G., 2016b. Preglacial to glacial sediment thickness grids for the Southern Pacific Margin of West Antarctica. *Geochemistry, Geophysics, Geosystems,* 17(10):4276–4285. **https://doi.org/10.1002/2016GC006401**

Lloyd, A.J., Wiens, D.A., Nyblade, A.A., Anandakrishnan, S., Aster, R.C., Huerta, A.D., Wilson, T.J., Dalziel, I.W.D, Shore, P.J., and Zhao, D., 2015. A seismic transect across West Antarctica: evidence for mantle thermal anomalies beneath the Bentley Subglacial Trench and the Marie Byrd Land Dome. *Journal of Geophysical Research: Solid Earth,* 120(12):8439–8460. **https://doi.org/10.1002/2015JB012455**

Lowe, A.L., and Anderson, J.B., 2002. Reconstruction of the West Antarctic Ice Sheet in Pine Island Bay during the Last Glacial Maximum and its subsequent retreat history. *Quaternary Science Reviews,* 21(16–17):1879–1897. **https://doi.org/10.1016/S0277-3791(02)00006-9**

Lowe, A.L., and Anderson, J.B., 2003. Evidence for abundant subglacial meltwater beneath the paleo-ice sheet in Pine Island Bay, Antarctica. *Journal of Glaciology,* 49(164):125–138. **https://doi.org/10.3189/172756503781830971**

McKay, R., Browne, G., Carter, L., Cowan, E., Dunbar, G., Krissek, L., Naish, T., et al., 2009. The stratigraphic signature of the late Cenozoic Antarctic Ice Sheets in the Ross Embayment. *Geological Society of America Bulletin,* 121(11–12):1537–1561. **https://doi.org/10.1130/B26540.1**

McKay, R., Naish, T., Carter, L., Riesselman, C., Dunbar, R., Sjunneskog, C., Winter, D., et al., 2012. Antarctic and Southern Ocean influences on late Pliocene global cooling. *Proceedings of the National Academy of Sciences of the United States of America,* 109(17):6423–6428. **https://doi.org/10.1073/pnas.1112248109**

McKay, R.M., De Santis, L., Kulhanek, D.K., Ash, J.L., Beny, F., Browne, I.M., Cortese, G., Cordeiro de Sousa, I.M., Dodd, J.P., Esper, O.M., Gales, J.A., Harwood, D.M., Ishino, S., Keisling, B.A., Kim, S., Kim, S., Laberg, J.S., Leckie, R.M., Müller, J., Patterson, M.O., Romans, B.W., Romero, O.E., Sangiorgi, F., Seki, O., Shevenell, A.E., Singh, S.M., Sugisaki, S.T., van de Flierdt, T., van Peer, T.E., Xiao, W., and Xiong, Z., 2019. Expedition 374 summary. *In* McKay, R.M., De Santis, L., Kulhanek, D.K., and the Expedition 374 Scientists, *Ross Sea West Antarctic Ice Sheet History.* Proceedings of the International Ocean Discovery Program, 374: College Station, TX (International Ocean Discovery Program). **https://doi.org/10.14379/iodp.proc.374.101.2019**

Milillo, P., Rignot, E., Rizzoli, P., Scheuchl, B., Mouginot, J., Bueso-Bello, J., and Prats-Iraola, P., 2019. Heterogeneous retreat and ice melt of Thwaites Glacier, West Antarctica. *Science Advances,* 5(1):eaau3433. **https://doi.org/10.1126/sciadv.aau3433**

Miller, K.G., Wright, J.D., Katz, M.E., Browning, J.V., Cramer, B.S., Wade, B.S., and Mizintseva, S.F., 2008. A view of Antarctic ice-sheet evolution from sea-level and deep-sea isotope changes during the Late Cretaceous–Cenozoic. *In* Cooper, A.K., Barrett, P.J., Stagg, H., Storey, B., Stump, E., Wise, W., and the 10th ISAES Editorial Team (Eds.), *Antarctica: A Keystone in a Changing World.* Proceedings of the 10th International Symposium on Antarctic Earth Sciences, 10:55–70. **https://pubs.usgs.gov/of/2007/1047/kp/kp06/of2007-1047kp06.pdf**

Minzoni, R.T., Majewski, W., Anderson, J.B., Yokoyama, Y., Fernandez, R., and Jakobsson, M., 2017. Oceanographic influences on the stability of the Cosgrove ice shelf, Antarctica. *The Holocene,* 27(11):1645–1658. **https://doi.org/10.1177/0959683617702226**

Muto, A., Peters, L.E., Gohl, K., Sasgen, I., Alley, R.B., Anandakrishnan, S., and Riverman, K.L., 2016. Subglacial bathymetry and sediment distribution beneath Pine Island Glacier ice shelf modeled using aerogravity and in situ geophysical data: new results. *Earth and Planetary Science Letters,* 433:63–75. **https://doi.org/10.1016/j.epsl.2015.10.037**

Naish, T.R., Powell, R., Levy, R., Wilson, G., Scherer, R., Talarico, F., Krissek, L., et al., 2009. Obliquity-paced Pliocene West Antarctic Ice Sheet oscillations. *Nature,* 458(7236):322–329. **https://doi.org/10.1038/nature07867**

Nitsche, F.O., Cunningham, A.P., Larter, R.D., and Gohl, K., 2000. Geometry and development of glacial continental margin depositional systems in the Bellingshausen Sea. *Marine Geology,* 162(2–4):277–302. **https://doi.org/10.1016/S0025-3227(99)00074-2**

Nitsche, F.O., Gohl, K., Larter, R.D., Hillenbrand, C.-D., Kuhn, G., Smith, J.A., Jacobs, S., Anderson, J.B., and Jakobsson, M., 2013. Paleo ice flow and subglacial meltwater dynamics in Pine Island Bay, West Antarctica. *The Cryosphere,* 7(1):249–262. **https://doi.org/10.5194/tc-7-249-2013**

Nitsche, F.O., Gohl, K., Vanneste, K., and Miller, H., 1997. Seismic expression of glacially deposited sequences in the Bellingshausen and Amundsen Seas, West Antarctica. *In* Cooper, A.K., Barker, P.F., and Brancolini, G. (Eds.), *Geology and Seismic Stratigraphy of the Antarctic Margin* (Part 2). Antarctic Research Series, 71:95–108. **https://doi.org/10.1029/AR071p0095**

Nitsche, F.O., Jacobs, S.S., Larter, R.D., and Gohl, K., 2007. Bathymetry of the Amundsen Sea continental shelf: implications for geology, oceanography, and glaciology. *Geochemistry, Geophysics, Geosystems,* 8(10):Q10009. **https://doi.org/10.1029/2007GC001694**

Padman, L., Fricker, H.A., Coleman, R., Howard, S., and Erofeeva, L., 2002. A new tide model for the Antarctic ice shelves and seas. *Annals of Glaciology,* 34:247–254. **https://doi.org/10.3189/172756402781817752**

Pagani, M., Liu, Z., LaRiviere, J., and Ravelo, A.C., 2010. High Earth-system climate sensitivity determined from Pliocene carbon dioxide concentrations. *Nature Geoscience,* 3:27–30. **https://doi.org/10.1038/ngeo724**

Paolo, F.S., Fricker, H.A., and Padman, L., 2015. Volume loss from Antarctic ice shelves is accelerating. *Science,* 348(6232):327–331. **https://doi.org/10.1126/science.aaa0940**

Parkinson, C.L., and Cavalieri, D.J., 2012. Antarctic sea ice variability and trends, 1979–2010. *The Cryosphere,* 6(4):871–880. **https://doi.org/10.5194/tc-6-871-2012**

Passchier, S., Browne, G., Field, B., Fielding, C.R., Krissek, L.A., Panter, K., Pekar, S.F., and ANDRILL-SMS Science Team, 2011. Early and middle Miocene Antarctic glacial history from the sedimentary facies distribution in the AND-2A drill hole, Ross Sea, Antarctica. *Geological Society of America Bulletin,* 123(11–12):2352–2365. **https://doi.org/10.1130/B30334.1**

Pollard, D., and DeConto, R.M, 2009. Modelling West Antarctic Ice Sheet growth and collapse through the past five million years. *Nature,* 458(7236):329–332. **https://doi.org/10.1038/nature07809**

Powell, R.D., and Cooper, J.M., 2002. A glacial sequence stratigraphic model for temperate, glaciated continental shelves. *In* Dowdeswell, J.A., and Ó'Cofaigh, C. (Eds.), *Glacier-Influenced Sedimentation on High-Latitude Continental Margins.* Geological Society Special Publication, 203:215–244. **https://doi.org/10.1144/GSL.SP.2002.203.01.12**

Rignot, E., Mouginot, J., Scheuchl, B., van den Broeke, M., van Wessem, M.J., and Morlighem, M., 2019. Four decades of Antarctic Ice Sheet mass balance from 1979–2017. Proceedings of the National Academy of Sciences. **https://doi.org/10.1073/pnas.1812883116**

Rocchi, S., LeMasurier, W.E., and Di Vincenzo, G., 2006. Oligocene to Holocene erosion and glacial history in Marie Byrd Land, West Antarctica, inferred from exhumation of the Dorrel Rock intrusive complex and from volcano morphologies. *Geological Society of America Bulletin,* 118(7–8):991–1005. **https://doi.org/10.1130/B25675.1**

Scherer, R.P., 2003. Quaternary interglacials and the West Antarctic Ice Sheet. *In* Droxler, A.W., Poore, R.Z., and Burckle, L.H. (Eds.), *Earth's Climate and Orbital Eccentricity: The Marine Isotope Stage 11 Question*. Geophysical Monograph, 137:103–112. **https://doi.org/10.1029/137GM08**

Scherer, R.P., Aldahan, A., Tulaczyk, S., Possnert, G., Engelhardt, H., and Kamb, B., 1998. Pleistocene collapse of the West Antarctic Ice Sheet. *Science,* 281(5373):82–85. **https://doi.org/10.1126/science.281.5373.82**

Scheuer, C., Gohl, K., and Eagles, G., 2006a. Gridded isopach maps from the South Pacific and their use in interpreting the sedimentation history of the West Antarctic continental margin. *Geochemistry, Geophysics, Geosystems,* 7(11):Q11015. **https://doi.org/10.1029/2006GC001315**

Scheuer, C., Gohl, K., Larter, R.D., Rebesco, M., and Udintsev, G., 2006b. Variability in Cenozoic sedimentation along the continental rise of the Bellingshausen Sea, West Antarctica. *Marine Geology,* 277(3–4):279–298. **https://doi.org/10.1016/j.margeo.2005.12.007**

Schoof, C., 2007. Ice sheet grounding line dynamics: steady states, stability, and hysteresis. *Journal of Geophysical Research: Earth Surface,* 112(F3):F03S28. **https://doi.org/10.1029/2006JF000664**

Smellie, J.L., Haywood, A.M., Hillenbrand, C.-D., Lunt, D.J., and Valdes, P.J., 2009. Nature of the Antarctic Peninsula Ice Sheet during the Pliocene: geological evidence and modelling results compared. *Earth-Science Reviews,* 94(1–4):79–94. **https://doi.org/10.1016/j.earscirev.2009.03.005**

Smith, J.A., Andersen, T.J., Shortt, M., Gaffney, A.M., Truffer, M., Stanton, T.P., Bindschadler, R., et al., 2017. Sub-ice-shelf sediments record history of twentieth-century retreat of Pine Island Glacier. *Nature,* 541(7635):77–80. **https://doi.org/10.1038/nature20136**

Smith, J.A., Hillenbrand, C.-D. Kuhn, G., Klages, J.P., Graham, A.G.C., Larter, R.D., Ehrmann, W., Moreton, S.G., Wiers, S., and Frederichs, T., 2014. New constraints on the timing of West Antarctic Ice Sheet retreat in the eastern Amundsen Sea since the Last Glacial Maximum. *Global and Planetary Change,* 122:224–237. **https://doi.org/10.1016/j.gloplacha.2014.07.015**

Smith, J.A., Hillenbrand, C.-D., Kuhn, G., Larter, R.D., Graham, A.G.C., Ehrmann, W., Moreton, S.G., and Forwick, M., 2011. Deglacial history of the West Antarctic Ice Sheet in the western Amundsen Sea Embayment. *Quaternary Science Reviews,* 30(5–6):488–505. **https://doi.org/10.1016/j.quascirev.2010.11.020**

Smith, R.T., and Anderson, J.B., 2010. Ice-sheet evolution in James Ross Basin, Weddell Sea margin of the Antarctic Peninsula: the seismic stratigraphic record. *Geological Society of America Bulletin,* 122(5–6):830–842. **https://doi.org/10.1130/B26486.1**

Spiegel, C., Lindow, J., Kamp, P.J.J., Meisel, O., Mukasa, S., Lisker, F., Kuhn, G., and Gohl, K., 2016. Tectonomorphic evolution of Marie Byrd Land—implications for Cenozoic rifting activity and onset of West Antarctic glaciation. *Global and Planetary Change*, 145:98–115. **https://doi.org/10.1016/j.gloplacha.2016.08.013**

Sutter, J., Gierz, P., Grosfeld, K., Thoma, M., and Lohmann, G., 2016. Ocean temperature thresholds for Last Interglacial West Antarctic Ice Sheet collapse. *Geophysical Research Letters,* 43(6):2675–2682. **https://doi.org/10.1002/2016GL067818**

Thoma, M., Jenkins, A., Holland, D., and Jacobs, S., 2008. Modelling Circumpolar Deep Water intrusions on the Amundsen Sea continental shelf, Antarctica. *Geophysical Research Letters,* 35(18):L18602. **https://doi.org/10.1029/2008GL034939**

Uenzelmann-Neben, G., and Gohl, K., 2012. Amundsen Sea sediment drifts: archives of modifications in oceanographic and climatic conditions. *Marine Geology,* 299–302:51–62. **https://doi.org/10.1016/j.margeo.2011.12.007**

Uenzelmann-Neben, G., and Gohl, K., 2014. Early glaciation already during the early Miocene in the Amundsen Sea, Southern Pacific: indications from the distribution of sedimentary sequences. *Global and Planetary Change,* 120:92–104. **https://doi.org/10.1016/j.gloplacha.2014.06.004**

Uenzelmann-Neben, G., Gohl, K., Larter, R.D., and Schlüter, P., 2007. Differences in ice retreat across Pine Island Bay, West Antarctica, since the Last Glacial Maximum: indications from multichannel seismic reflection data. *In* Cooper, A.K., Raymond, C.R., et al. (Eds.), *Antarctica: A Keystone in a Changing World—Online Proceedings of the 10th International Symposium on Antarctic Earth Sciences.* USGS Open-File Report 2007-1047, Short Research Paper 084. **https://pubs.usgs.gov/of/2007/1047/srp/srp084/of2007-1047srp084.pdf**

Vaughan, D.G., 2008. West Antarctic Ice Sheet collapse—the fall and rise of a paradigm. *Climate Change,* 91(1–2):65–79. **https://doi.org/10.1007/s10584-008-9448-3**

Villa, G., Persico, D., Wise, S.W., and Gadaleta, A., 2012. Calcareous nannofossil evidence for Marine Isotope Stage 31 (1 Ma) in Core AND-1B, ANDRILL McMurdo Ice Shelf Project (Antarctica). *Global and Planetary Change,* 96–97:75–86. **https://doi.org/10.1016/j.gloplacha.2009.12.003**

Walker, D.P., Brandon, M.A., Jenkins, A., Allen, J.T., Dowdeswell, J.A., and Evans, J., 2007. Oceanic heat transport onto the Amundsen Sea shelf through a submarine glacial trough. *Geophysical Research Letters,* 34(2):L02602. **https://doi.org/10.1029/2006GL028154**

Warny, S., Askin, R.A., Hannah, M.J., Mohr, B.A.R., Raine, J.I., Harwood, D.M., Florindo, F., and the SMS Science Team, 2009. Palynomorphs from a sediment core reveal a sudden remarkably warm Antarctica during the middle Miocene. *Geology,* 37(10):955–958. **https://doi.org/10.1130/G30139A.1**

Weigelt, E., Gohl, K., Uenzelmann-Neben, G., and Larter, R.D., 2009. Late Cenozoic ice sheet cyclicity in the western Amundsen Sea Embayment—evidence from seismic records. *Global and Planetary Change,* 69(3):162–169. **https://doi.org/10.1016/j.gloplacha.2009.07.004**

Wellner, J.S., Lowe, A.L., Shipp, S.S., and Anderson, J.B., 2001. Distribution of glacial geomorphic features on the Antarctic continental shelf and correlation with substrate: implications for ice behavior. *Journal of Glaciology,* 47(158):397–411. **https://doi.org/10.3189/172756501781832043**

Wilch, T.I., McIntosh, W.C., and Dunbar, N.W., 1999. Late Quaternary volcanic activity in Marie Byrd Land: potential $^{40}Ar/^{39}Ar$-dated time horizons in West Antarctic ice and marine cores. *Geological Society of America Bulletin,* 111(10):1563–1580. **https://doi.org/10.1130/0016-7606(1999)111<1563:LQVAIM>2.3.CO;2**

Wilson, D.S., Jamieson, S.S., Barrett, P.J., Leitchenkov, G., Gohl, K., and Larter, R.D., 2012. Antarctic topography at the Eocene-Oligocene boundary. *Palaeogeography, Palaeoclimatology, Palaeoecology,* 335–336:24–34. **https://doi.org/10.1016/j.palaeo.2011.05.028**

Wilson, D.S., and Luyendyk, B.P., 2009. West Antarctic paleotopography estimated at the Eocene–Oligocene climate transition. *Geophysical Research Letters,* 36(16):L16302. **https://doi.org/10.1029/2009GL039297**

Wilson, D.S., Pollard, D., DeConto, R.M., Jamieson, S.S.R., and Luyendyk, B.P., 2013. Initiation of the West Antarctic Ice Sheet and estimates of total Antarctic ice volume in the earliest Oligocene. *Geophysical Research Letters,* 40(16):4305–4309. **https://doi.org/10.1002/grl.50797**